CHEMISTRY
AN ASIAN JOURNAL

www.chemasianj.org

A Journal of

ACES
Asian Chemical Editorial Society

REPRINT

WILEY-VCH

ACES Asian Chemical Editorial Society

doi.org/10.1002/asia.202100516

CHEMISTRY AN ASIAN JOURNAL Minireview

Special Collection

Micro-droplet Trapping and Manipulation: Understanding Aerosol Better for a Healthier Environment

Yuan-Pin Chang,*[a, b] Yanita Devi,[a] and Chun-Hu Chen*[a]

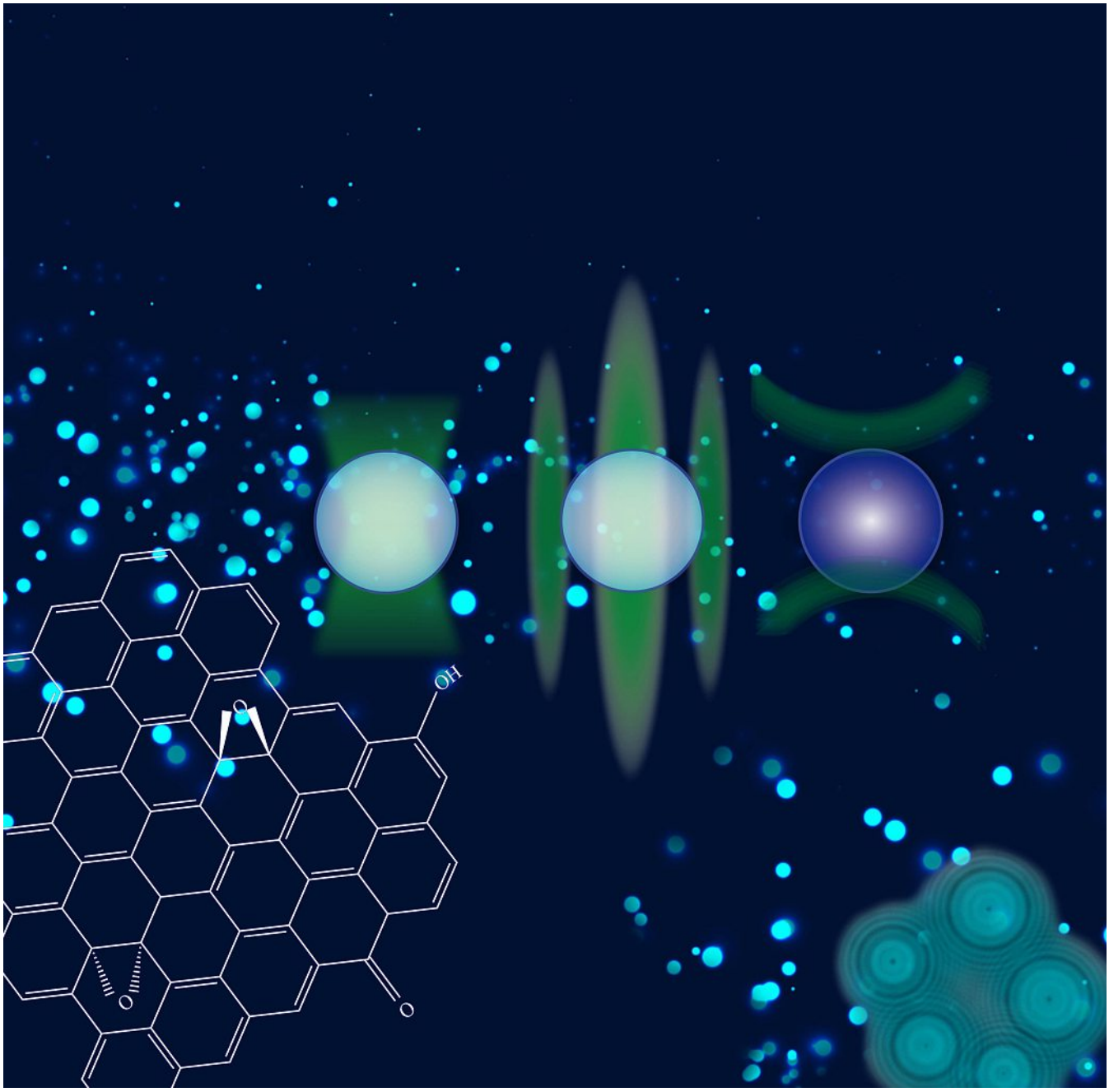

Abstract: Understanding the physicochemical properties and heterogeneous processes of aerosols is key not only to elucidate the impacts of aerosols on the atmosphere and humans but also to exploit their further applications, especially for a healthier environment. Experiments that allow for spatially control of single aerosol particles and investigations on the fundamental properties and heterogeneous chemistry at the single-particle level have flourished during the last few decades, and significant breakthroughs in recent years promise better control and novel applications aimed at resolving key issues in aerosol science. Here we propose graphene oxide (GO) aerosols as prototype aerosols containing polycyclic aromatic hydrocarbons, and GO can behave as two-dimensional surfactants which could modify the interfacial properties of aerosols. We describe the techniques of trapping single particles and furthermore the current status of the optical spectroscopy and chemistry of GO. The current applications of these single-particle trapping techniques are summarized and interesting future applications of GO aerosols are discussed.

1. Motivation

During the last few decades, scientists started to exploit the unique chemistry of aerosols, such as in the fields of atmospheric chemistry, interface chemistry, and material chemistry.[1] Aerosols are solid, semi-solid or liquid particles suspended in the gaseous environment with diameter from 1 nm to 100 μm. As aerosols have significantly large surface-to-volume ratios, the chemistry of aerosols is dominated by both the bulk reaction and the chemistry on the surface or interface, as depicted by Figure 1. For the bulk reactions which include the reactions of both solvated species, the kinetics in aerosols are not only determined by the liquid-phase reaction rates but also the diffusion kinetics, which are associated with the viscosity of the droplet.[2] The aerosol viscosity can be further affected by the hygroscopicity of solutes, which can determine the equilibrium size of the droplet and thus the solute strengths. Solute strengths can affect the liquid-phase bimolecular reaction rates and thus liquid-phase reaction kinetics.[3] Recently, Abbatt et al. found that the extraordinary large solute strengths in some atmospheric aerosols can significantly enhance the rate of the reaction of SO_2 and hydrogen peroxide.[4] Therefore, even the bulk reactions of aerosols can be significantly influenced by the interactions between aerosols and gaseous environments. To further understand and to exploit the chemistry of aerosols, it is necessary to elucidate the interplays between these physicochemical properties of aerosols.[5]

The interface reactions in aerosols include the reactions of gaseous species and species at the interface or the reactions of both species at the interface. The reactions at the interface could be different from those in the bulk because of following interface effects. As the intermolecular interactions with the solvent molecules at the interface, where only the half of the solute molecule is surrounded by solvent molecules, are significantly different from those in the bulk, where the entire solute molecule is surrounded by solvent molecules. As a result, the electronic potential of the species at the interface may be different from those in the bulk or in gas phase, modifying the reactivity of the solute species at the interface.[6] The molecules at the interface could also have a preferred spatial orientation, which could further affect their reactivities at the interface due to the steric effects. Furthermore, the diffusion coefficients, concentration gradients and pH values at the interfaces could be different from those in the bulk,[7] again affecting the kinetics or the reaction pathways at the interfaces. Recently, Wang et al. found that the pH near the aerosol surfaces could be significantly different from that of the bulk of aerosols,[7c,d, 8] suggesting the possible existence of a pH gradient near the air-water surfaces of aerosols. The studies of Enami et al. have focused on exploiting the modified reactivities at the air-water interfaces of aerosols (few μm in diameter).[9] The reaction of ascorbic acid with ozone near the air-water interface was found to be several hundred times faster than that in the bulk.[9a] Their study of the oxidation reaction of uric acid with ozone even found that the reactivities of uric acid in micro-droplets at different pH are significantly modified, completely different

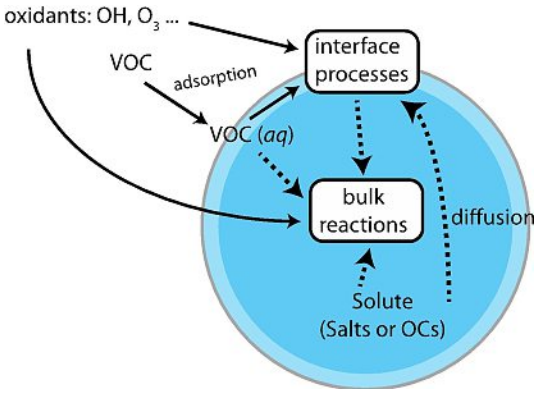

Figure 1. Representative scheme of heterogeneous oxidation reactions of organic compounds (OCs) or volatile OCs (VOC) in aerosol phase. (Adapted with permission from ref. 6a, Copyright 2012 Wiley-VCH.) Dashed arrows represent the diffusions inside the droplet. Solid arrows indicate the movements or physical processes of molecules in gas phase or on the interface of the droplet.

[a] *Prof. Y.-P. Chang, Y. Devi, Prof. C.-H. Chen*
Department of Chemistry
National Sun Yat-sen University
No. 70 Lien-hai Rd., Kaohsiung 80424 (Taiwan)
E-mail: ypchang@mail.nsysu.edu.tw
chunhu.chen@mail.nsysu.edu.tw
[b] *Prof. Y.-P. Chang*
Aerosol Science Research Center
National Sun Yat-sen University
No. 70 Lien-hai Rd., Kaohsiung 80424 (Taiwan)
This manuscript is part of a Special Collection dedicated to Early Career Researchers.

from pH-independent rates reported for this reaction in bulk water.[9d] Their studies of alkene ozonolysis also found that the reaction intermediates can exist at the air-water interfaces, while they are highly reactive toward water.[9a–c]

In the field of mass spectrometry, there has be extensive studies about the acceleration of organic reactions in micro-droplets, which are utilized as wall-less micro-reactors with small compartments and large surface areas.[10] Recently Zare and co-workers exploited the chemistry of micro-droplets via electrospray ionization mass spectrometry. They utilized a theta capillary to facilitate rapid mixings of two liquid-phase reactants, and these reactants ejected from the capillary are subsequently fused into micro-droplets (average few μm in diameter) where the reactions start to occur. They found that several fundamental reactions carried out in micro-droplets can be accelerated from a few times to ever several order of magnitudes.[11] For hydrogen-deuterium exchange reactions of phenethylamine in aqueous droplets, the observed rates of H–D exchange were found to be 3 times faster than those reported from bulk measurements.[11a] For the case of the cycloaddition reaction of diethyl azodicarboxylate and quadricyclane, the rate of the reaction in aqueous micro-droplets is accelerated by a factor of 10^2 compared to that reported from bulk measurements.[12] The mechanism of the acceleration in droplets is typically illustrated in terms of free energy lowering or modified reactivities at the interface, as described in the previous paragraph. However, such explanation still needs to be experimentally verified in details. Recently, Wilson et al. utilized a branched quadrupole trap to study the reaction of o-phthalaldehyde with alanine in a single droplet with around 40 μm in diameters, and they found that their reaction rate is slightly faster (~25%) in a droplet than in bulk solution, due to larger surface to volume ratio of the droplet compared to the bulk. However, they claimed that charges on the droplet and the enriched concentration of reactants due to evaporation do not play a significant role in any potential rate enhancement for their case. On the other hand, some of droplet-accelerated reactions may be explained in terms of charge transfer occurred at or near the surface. Zare et al. have found that hydrogen peroxide can be spontaneously generated from pure water micro-droplets, and they proposed that H_2O_2 may be generated from self-reactions of OH radicals, which are generated from OH^- losing electrons due to pH gradient and electric field at the surface.[13] Finally, Zare et al. found that pure water micro-droplets can spontaneously reduce several organic molecules without any added electron donors or acceptors and without any applied voltage, while none of these reactions occurs spontaneously in bulk water.[14]

In recent years, the aerosol technology has also been developed as a novel method to produce nano-size or nano-structure materials.[15] Zare et al.[11e] found that the micro-droplet fusion can synthesize gold nanoparticles or nanowires without reducing agents or templates, and such method can also accelerate the growth rate by a factor of about 10^5, compared to bulk solution. The aerosol technology can also allow for folding or reshaping two-dimensional (2D) sheet materials, such as graphene or graphene oxide (GO), to three-dimensional (3D) structures or hybrid composites which could exhibit distinct properties. Zangmeister et al.[15g] demonstrated that GO can be reshaped as crumpled nanopaper-like sheet via rapidly drying aqueous GO aerosols. Hunt et al.[15f] demonstrated that GO in water droplets can segregate into cargo-filled nanosacks upon drying aerosols. Fortner et al.[15i] utilized water evaporation-induced confinement forces inside aerosols to synthesize crumpled graphene-TiO_2-magnetite nanocomposite photocatalysts. Jabari and Toyserkani exploited an aerosol-jet technique to print graphene interconnects.[15h] Recently, Tsai et al.[16] utilized such aerosol-based synthetic approach to fabricate GO or reduced GO (RGO) nanocomposites with silsesquioxane or MnO_x via gas-phase evaporation-induced self-assembly inside precursor aerosols. Zhu et al.[17] also utilized the similar aerosol spray-freezing method where precursor droplets were rapidly freezed by liquid nitrogen to fabricate a kind of 3D architectural hybrid, composed of RGO and ultrathin MoS_2 layers. Finally, Woźniak et al. demonstrated that dryind microdroplets of colloidal suspension can lead to the formation of highly ordered 3D spherical quasi-crystals which cannot be formed from the aggregation on a substrate.[15d,18]

Yuan-Pin Chang received his D. Phil. degree in Physical Chemistry at University of Oxford in 2010. He then worked as post-doctoral at Center of Free Electron Laser Science, DESY, Hamburg in 2011, and at Institute of Atomic and Molecular Science, Academia Sinica, Taipei in 2015. He then joined the Department of Chemistry at National Sun Yat-sen University in 2017 as an Assistant Professor. His research interests include reaction kinetics of aerosol, optical trapping, and aerosol LIDAR.

Yanita Devi received her Batchelor degree in Chemical Engineering at Widya Mandala Catholic University Surabaya Indonesia in 2020. Right now, she is a master student at the Department of Chemistry at National Sun Yat-sen University under supervision of Prof, Chun-Hu Chen.

Chun-Hu Chen received his PhD degree in Chemistry at University of Connecticut in 2010. He conducted his post-doctoral career in Material Science and Engineering at The Ohio State University. He is currently a Professor of Chemistry Department at National Sun Yat-sen University since 2020. His research interests focus on graphene 2-D materials and semiconductor metal oxides for clean energy and environmental applications.

The chemistry of aerosols can have a significant impact on health effects of human and ecosystems. Polycyclic aromatic hydrocarbons (PAHs) are main toxic sources of anthropogenic or polluted atmospheric aerosols, as PAHs in air are mostly in condensed phase due to their low vapor pressures. PAHs are notorious toxic air pollutants, as they can cause carcinogenic and mutagenic effects.[19] The toxicity of PAH aerosols is further modified by heterogeneous reactions with ozone, but the reaction mechanism and kinetics are not fully clarified yet.[20] A recent study investigated the multi-phase reactivities of PAHs in thin films toward gaseous ozone, and the findings show that the formation of secondary organic aerosol (SOA) reaction products can result in SOA-PAH phase separation and slow diffusions of interior PAHs toward the film surface, prolonging the chemical lifetime of PAHs.[20] Such inefficient chemical degradation due to the slow diffusion of PAHs inside SOA becomes one of main reasons resulting in the long-range transport of these persistent PAHs.[21]

Finally, micro-droplets can be utilized as prototype system of thin-film liquids on bio-surfaces, facilitating laboratory investigations of interfacial biochemistry. Enami et al. have utilized micro-droplets as model system of air-water interfaces to study the interfacial reactions between antioxidants in lung lining fluids, such as ascorbic acid and uric acid, and atmospheric oxidants, such as ozone.[9a,d] For the case of aqueous ascorbic acid aerosol ozonolysis, they found that the high acidities can enhance the formation of a persistent ascorbic acid ozonide near the air-water interface, which can further transduce oxidative damages toward bio-surfaces.[9a] As described before, they also found that the reaction of interfacial uric acid with ozone exhibits a significant pH dependence.[9d] Recently, Chang et al. utilized aqueous ascorbic acid micro-droplets as prototype bioaerosols to investigate the kinetics of their reactions with gaseous ozone by means of aerosol optical tweezers.[22] They found that the reactivities of ascorbic acid in aqueous aerosols toward ozone are significantly dependent on aerosol pH and ion strength, and high acidities could significantly reduce the reactivity of ascorbic acid toward ozone. These findings suggest that the enhanced acidity of airway lining fluids due to inhaled sulfur dioxide or acidic particular matters can suppress the antioxidant activity and cause more direct contacts of atmospheric oxidants to bio-surfaces.[22] These ascorbic acid or uric acid aerosols can also be regarded as prototype bio aerosols, and these antioxidants actually could become to protect the pathogens inside bio-aerosols against ozone from environments for a period of time. As a result, the lifetime of pathogens in bio-aerosols could also be correlated to the oxidation reaction kinetics of aerosols.[22]

2. Technique background

The spatial control of aerosol particles provides several advantages for elucidating and manipulating the dynamic processes in the aerosol with unprecedented details and accuracies. At first, it allows for investigating the aerosol chemistry *in situ*, because it can facilitate contactless measurements of aerosol particles suspended under controlled gaseous environments, without any interference of substrate surface.[1b] Such wall-less experiment for aerosols can also significantly simplify the experimental implementation of preparing and investigating highly oversaturated or super-cooled liquid state.[23] Furthermore, as the trapped aerosol particles can be spatially confined for a long period of time, such as over tens of hours, the precision measurements of single aerosol spectroscopy and the full investigations of various dynamical processes in different time scales can be carried out. Furthermore, the techniques of trapping single aerosol particles can be coupled with several novel spectroscopic methods that allow for determining various physical and chemical properties of the trapped aerosol particles. Thus, the interplays between the physicochemical properties of the aerosol and heterogeneous/multiphase processes of the aerosol can be fully elucidated. To gain a spatial control of condensed phase particles, particularly for the particles in size of few μm, the optical trapping and electrodynamic balances techniques dedicated to aerosol measurements have been developed and utilized extensively. There are already several reviews that provide comprehensive accounts of these single aerosol particle trapping techniques.[24] Thus, in the following sections we will briefly introduce the techniques and summarize the recent progresses of their applications in single aerosol measurements. While acoustic traps are also extensively utilized to study the interface chemistry and chemistry of micro-particles,[25] we will not describe it here, because of the limited range of particle sizes (at least over few tens μm in diameter) can be trapped by this technique.

Finally, while this review focuses on the works of trapping aerosol particles, It should be noted that various microfluidic concepts and tools have also been developed to trap or manipulate single emulsion droplets, promising potential applications to aerosol science, such as single-particle studies of microphysical properties and heterogeneous chemistry.[26]

2.1. Optical trapping of aerosols

One of optical trapping techniques, so called "optical tweezers", has been firstly developed by Ashkin *et al.* since 1986.[27] The optical tweezers provides a robust trap with the optical gradient force significantly larger than the scattering and gravitational forces, leading to a three-dimensional confinement of a dielectric particle in position with a single laser beam,[28] as shown in Figure 2 (a). This strategy is typically achieved by utilizing a microscope objective of a high numerical aperture to generating a highly focused Gaussian laser beam. Particles with sizes ranging from microns down to hundreds of nanometers can be steadily trapped and positioned with a high precision. The optical tweezers experiments are usually performed in liquid environments, such as the extensive applications in biological and colloidal sciences. There were also numerous experimental attempts for optical trapping of particles in gaseous environments,[29] while forming a stable trap for aerosols is a more challenging task because of the larger

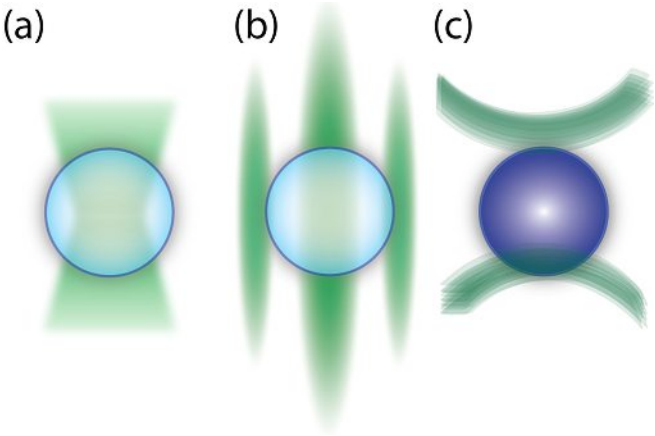

Figure 2. Schematics of three types of optically trapping aerosol particles. (a) Gradient force trapping via Gaussian beam, (b) Gradient force via zero-order Bessel beam and (c) photophoretic force trapping via hollow beam. For the first two cases, the downward gravitation force is balanced by the gradient force and the scattering force which pushes particles upward. For the last case, the gravitation force is balanced by the photophoretic force pushing the particle upward.

density contrast between particle and medium.[28a,29b,30] Optical trapping of particles, particularly aqueous micro-droplets, in air can facilitate various novel applications in atmospheric chemistry, aerosol science and interfacial chemistry, and these applications promise to answer several key questions in these fields.[24a]

Tweezing single water micro-droplets in air was firstly realized by Reid et al.[24h,31] and Ward et al.[32] And since then, the extensive applications of this aerosol optical tweezers (AOT) start to emerge in the fields of aerosol chemistry and spectroscopy, because of the simplicity of this experimental design and the fundamental importance of aqueous aerosols in atmospheric chemistry.[33] To form a stable optical trap for aqueous micro-droplets, they utilized a single-beam configuration where the focused laser beam propagated upwards, so that the scattering force from the laser beam can cancel out the gravitational force, as depicted in Figure 2 (a). In some literature, such trapping strategy is also called optical levitation,[28a] as one can even tune the laser power and adjust the equilibrium height of the particle over the range of few micrometers.[33a] The size of particles which can be trapped by AOT ranges from 4 to 14 μm in diameter.[31] The laser wavelength used for tweezing liquid droplets is typically in the visible to near infrared regions, because of relatively low absorption coefficients of water at these wavelengths. The typical laser power for trapping a single micro-droplet *via* single-beam AOT is about few mW, which only causes a negligible effect of laser heating (<1 K).[31,34] Recently, more advanced optical traps for aerosols utilized counter-propagating dual beams with equal powers to trap single aerosol particles, where two opposite scattering forces will cancel each other out. Therefore, this dual-beam configuration allows for using significantly large trapping laser powers (few hundreds mW) for various advanced applications.[23a,35] Recently, Ward et al. demonstrated the optical trapping of solid particles and pharmaceutical aerosols via dual-beam AOT.[36]

Analyzing the Raman signals of the optically trapped micro-droplet excited by the tightly focused trapped laser can be a powerful and sensitive spectroscopic means to retrieve its microphysical properties.[37] Figure 3 shows the typical Raman spectra of the single trapped micro-droplets, which contain molecular Raman signals (aqueous citric acid in this case) and relatively sharp cavity-enhanced Raman scattering (CERS) signals, which are the whisper gallery mode resonances of stimulated Raman scattering inside the spherical droplet behaving as an optical cavity.[38] As the CERS signals of each droplet are sensitive to its morphology, the analysis of CERS spectra allows for the determination of its radius and complex refractive index (RI) with high precisions and in real time.[24i,39] The typical standard deviations of fitted radius and RI derived from the simulations of CERS wavelengths based on Mie theory can be down to $<\pm 2$ nm and $<\pm 0.0005$, respectively.[40] Such sensitive spectroscopic means facilitates the AOT method to

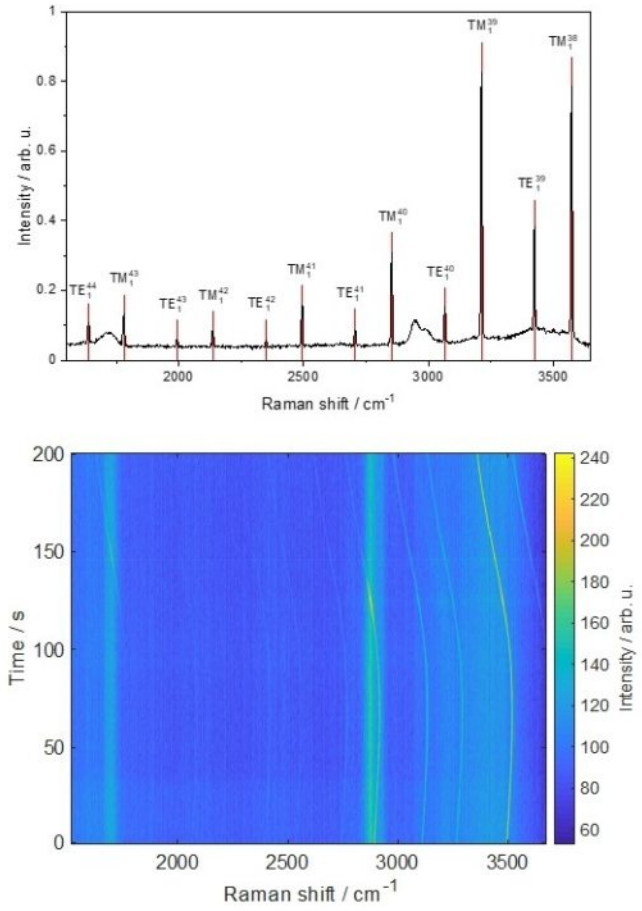

Figure 3. (Top) Representative Raman spectrum of an optically trapped aqueous citric acid droplet (black line) and the fit to the CERS signals (red line) along with assignments of whisper gallery modes. The fit was performed by *mrfit* program developed by Preston et al.[39b] The fitted radius is 3.281 μm. (Bottom) Raman spectra time series for the trapped citric acid droplet. The color scale indicates the intensity of the Raman signal. The relatively bright curved lines are CERS signals. The blue shifts of CERS signals indicate the decrease of radius, because of water evaporation.

investigate various fundamental properties and processes of aerosols in details, such as the mass and heat transfer at a liquid water surface,[41] the coagulation and growth processes of the aerosol[39c,40,42] and the vapor pressures, hygroscopicities and other thermodynamical properties of aerosols containing semi-VOCs,[43] via measuring the changes of the droplet volume and RI during the evaporations of VOCs and water. Preston et al. utilized the dual-beam AOT with large laser powers to induce a significant laser heating in trapped droplets, allowing for determining the imaginary part of RI.[35a] Besides the radius and RI, the pattern of CERS signals also depends on the morphology of the droplet, and thus they can also be utilized to characterize the phase segregation of immiscible organic and inorganic components within single droplets and their corresponding morphology,[44] deformation of droplet shapes[34] and core-shell structures of SOA and glassy aerosol particles.[45] Finally, besides CERS, the broadband Mie scattering signals from single particles which were illuminated with a broadband light source can also be used to determine the corresponding radius and RI, and this technique promises to yield more Mie resonances and thus better fits than those from CERS.[35b,46]

AOT coupled with time-resolved spectroscopic means allows for elucidating the dedicated interplays between the kinetic, microphysical and thermodynamic properties of the heterogeneous/multiphase reactions of aerosols, such as the heterogeneous oxidation reactions of single aqueous inorganic/organic acid aerosol particles with gaseous ozone.[22,43d,e,47] Sullivan at al. utilized AOT to demonstrate the first capture and analysis of SOA on a suspended droplet which was exposed in the gas-phase reaction of α-pinene and ozone. Such synthesized SOA particles have core-shell morphologies, and the growth process and microphysical properties of the SOA shell, such as thickness and diffusivity, can been fully characterized by CERS spectroscopy.[45d,48] Reid et al. utilized AOT to explore the influence of organic films on the evaporation and condensation of water in aerosol.[49] The photochemistry of single airborne micro-droplets were also investigated via AOT.[50] Tobon et al. combined AOT and Raman microspectroscopy to study the photolysis of aqueous $NaNO_3$ droplets and the spatial distributions of photoproducts within the droplet can be determined.[50a] Seng et al. utilized AOT to investigate the deliquescence behavior of photo-irradiated single $NaNO_3$ droplets, which are significantly affected by photoproducts.[50b]

The molecular Raman signals can be used to determine not only the chemical composition but also the pH of individual aqueous droplets with high accuracies. Numerous chemical reactions of VOCs associated with generating SOA can be affected by particle-phase acidity.[51] However, determining the pH of aerosols and clarify its effects are still challenging tasks in the field of atmospheric aerosols.[52] Here the basic principle is to measure the Raman intensity ratios of conjugate acid/base pairs in aerosols, and then the aerosol pH can be determined from comparing with the calibration curves of Raman ratio versus pH established from bulk measurements.[53] However, in order to correctly predict pH ($=-\log(a_{H^+})$) of aerosols, which could also have relatively high ionic strengths, the effect of non-ideal thermodynamics associated with high ionic strengths to the proton activity has to be taken into account.[53,54] Ault et al. utilized Raman microspectroscopy and pH indicator paper method to determine the pH of aerosol particles impacted onto substrates.[53,55] Grassian et al. utilized AOT coupled with Raman spectroscopy and sulfate/bisulfate and carbonate/bicarbonate as model systems, and the pH changes of a single trapped micro-droplet can be precisely determined during its coalescence with strong acid aerosols.[54a] Sullivan et al. utilized sulfate/bisulfate to determine the pH of single picoliter droplets over a range of -0.36 to 0.76 with the uncertainties ranging from ± 0.03 to 0.06.[54b] Very recently, Chang et al. utilized hydrogen phosphate/dihydrogen phosphate to maintain the pH of single micro-droplets at around 6, and they also used the Raman intensities of phosphates to monitor the aerosol pH over a range of about 5.5 to 7.3, during the reaction of aqueous ascorbic acid micro-droplets with gaseous ozone.[22] Figure 4 shows the Raman spectra of single aqueous ascorbic acid aerosol particle at pH$\approx$6 before and after exposed to ozone. The Raman peaks attributed to or coupled to the C=H bond of ascorbic acid disappeared after the reaction with ozone. The relative Raman intensities of hydrogen phosphate and dihydrogen phosphate remained the same during the reaction, indicating no significant change of pH.[22] However, they did not consider the effect of high ionic strengths inside micro-droplets, and the deviations of pH could be up to about one unit.[56]

Recently, several advanced AOT technologies were developed to measure the viscosity or diffusion coefficient of single aerosol particles, as these properties can have profound influences to fundamental dynamic processes of aerosols.[2b,57] Figure 5 shows the effect of diffusion rate to the kinetics of the reaction of condensed-phase species in a spherical particle and gaseous phase species which continuously dissolves into this particle via its interface. According to Stokes-Einstein equation, viscosity is inversely proportional to diffusion coefficient. Thus,

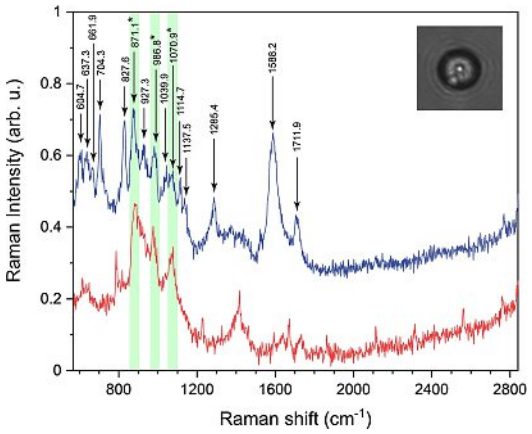

Figure 4. Representative Raman spectra of an optically trapped aqueous ascorbic acid droplet in pH$\approx$6 before (top data in black line) and after (bottom data in red line) the reaction with ozone at 85% RH, adapted from Ref. [22]. Two spectra are offset for clarity. The inset shows the brightfield image of the droplet before the reaction with ozone. The peak assignments (arrows with wavenumbers) without asterisk belong to aqueous ascorbic acid, and three peak assignments with asterisks and green marks belong to phosphates. Note that the relatively sharp peaks in the spectra, particularly in the spectrum after the reaction, are CERS signals.

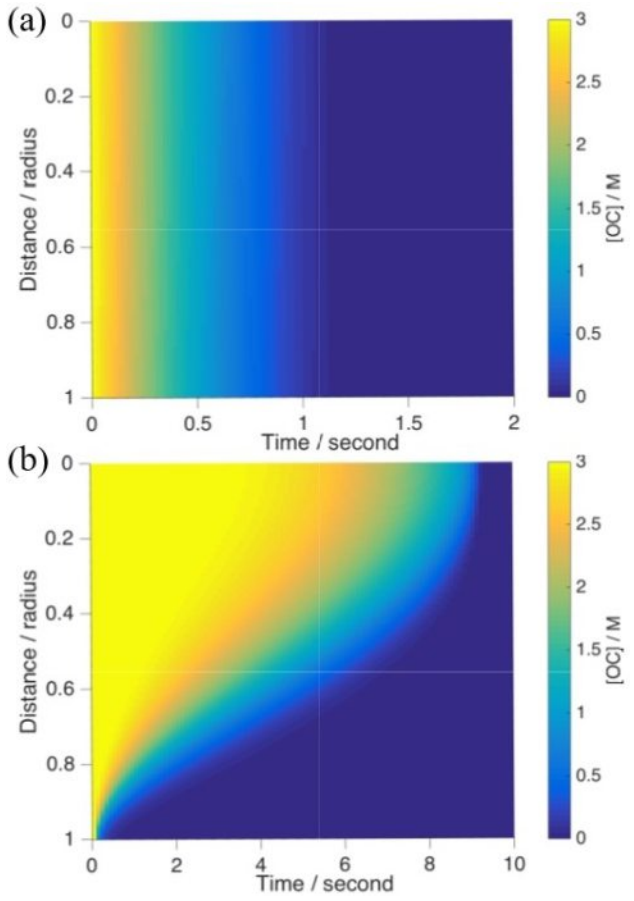

Figure 5. Calculated concentration profiles of condensed-phase species OC, as a function of time and position within the particle (radius = 1 μm) exposed to gaseous reactants, when OC has (a) fast diffusion ($D_{OC} = 1 \times 10^{-7}$ cm^2 s^{-1}) and (b) slow diffusion ($D_{OC} = 1 \times 10^{-10}$ cm^2 s^{-1}). (Adapted with permission from Ref. [57b], Copyright 2003 American Chemical Society.)

small viscosities can result in fast diffusion rates, and the reaction inside the droplet becomes more or less homogeneous, as depicted by Figure 5(a). However, large viscosities can result in slow diffusion rates, causing slower reaction rates inside the droplet and a large concentration gradient, as depicted by Figure 5(b).[57b] Individual aerosol particles which have different phases and compositions can have significantly different viscosities, and thus it is necessary to measure the viscosity of each single aerosol particle. Reid and McGloin et al.[2b,24f,58] have developed a holographic optical tweezers which can optically trap multiple aerosol particles at the same time and also manipulate their motions. They utilized this technique to perform coalescence events of two trapped droplets and determined the oscillating frequencies and damped timescale of the oscillating coalesced droplet, which are related to its surface tension and viscosity, respectively.[58c,59] Thus, this method can determine the viscosity of micro-droplets over a broad range of 12 orders of magnitude (10^{-3} to 10^{9} Pa s), including dilute aqueous solutions to semisolids.[59b] Also, the measured surface tensions of optically trapped aerosols via this method agree with those obtained from bulk tensiometry.[59c]

On the other hand, Fitzgerald et al. developed a non-destructive technique of probing the viscosity of aerosols which combines dual-beam AOT and fluorescent lifetime imaging microscopy.[60] The basic principle of this method is to measure the fluorescence time profiles of dye molecules as molecular rotors inside the droplet, and the fluorescence lifetimes can be used to derive the viscosity of the environment around the dye molecules. This technique can determine the viscosity over a range of 5 orders of magnitude (10^{-3} to 10^{2} Pa s), and it can even allow for mapping the viscosity of all positions on the trapped aerosol particle. They further monitored the dynamic change of the microscopic viscosity of organic aerosol particles subjected to the oxidation via ozone and hydroxyl radicals.[61] When the aging particle was transformed from liquid to solid phase, they observed the significant increase of viscosity. Recently, Reid et al.[47d,62] exploited the volatilization and ozonolysis of maleic acid in ternary aerosol particles containing water and sucrose as a model system to investigate the interplay between the mass transfer processes and viscosity of aerosol. They demonstrated that the aerosol viscosity indeed can significantly affect the vapor pressure of maleic acid and its reaction kinetics, and the Stokes-Einstein equation for organic molecules, such as maleic acid, keeps valid in such system where the matrix molecules, i.e., sucrose, have the similar sizes of organic molecules.[47d,62] However, they found that for viscous aerosol the measured aerosol viscosity and the corresponding diffusion coefficients of water do not agree with the Stokes-Einstein equation, and the disagreement could be over one order of magnitude.[59b,62,63] According to molecular dynamics simulations, the matrix formed by large molecules in viscous aerosol particles could pack less efficiently, facilitating a mechanism for small molecules such as water to tunnel through such porous network and thus increasing the divergence from Stokes-Einstein predictions for small molecules.[63]

Strictly speaking, the Stokes-Einstein equation is only valid in the case of large spherical molecules diffusing in a dilute solution.[64] Aerosol particles typically have concentrated chemical species, and some of atmospheric aerosols may be in the super-cooled phase, where the Stokes-Einstein could be invalid.[65] Thus, it is also necessary to measure the diffusion coefficient inside aerosol droplets directly. The AOT method has been coupled with various spectroscopic techniques to determine the diffusion coefficients of single micro-droplets. Krieger et al. utilized AOT coupled with CERS spectroscopy to investigate the influence of water diffusion to the mass transfer of water in glassy aerosol.[66] Davies and Wilson utilized the method of isotopic exchange of H_2O/D_2O to determine water diffusion coefficients over a wide range (10^{-12}–10^{-17} m^2 s^{-1}) in highly viscous states of optically trapped droplets.[67] Preston et al. measured the diffusion coefficients of a binary particle containing a volatile and a non-volatile component via measuring the frequency-dependent response (e.g. change in radius) of the particle when subjecting to oscillations of one of its chemical components in the gas phase.[68] Very recently, Miura et al. combined AOT and polarized Raman microspectroscopy to determine the rotational relaxation (diffusion) time from the Fourier transform of the Lorenz fits to the observed

Raman peaks of super-cooled dimethylsulfoxide droplets. They determined the temperature dependence of viscosity, and they found that the viscosity of super-cooled dimethylsulfoxide droplets is significantly higher than that in bulk.[23b]

The AOT technology can also facilitate contactless tensiometry measurements of single aqueous aerosol particles and thus determine their surface tensions. The surface tension can play an important role in the cloud formation process, and the effect of interfacial organics to the adsorption dynamics of the droplets is still a fundamental issue in geochemistry.[69] Dutcher et al. utilized holographic optical tweezers to measure the surface tensions of aqueous droplets of five ternary systems and established a thermodynamic model for aerosol surface tension.[70] Furthermore, Prisle et al. utilized the same technique to demonstrate that the surfactants can significantly reduce the surface tension of micro-droplets below the value of water, and such surface tension reduction is droplet size dependent.[71] Endo et al. utilized AOT combined with the quasielastic light scattering method[72] to measure the resonant frequencies of thermally induced capillary-waves on the spherical liquid surface of the trapped droplets, and these resonant frequencies can be used to derive the surface tension of droplets.[73] Very recently, Preston et al. utilized a dual-beam AOT to realize the nanometer-scale optical deformations on aqueous microdroplets, and such small change in shape can be measured using CERS spectroscopy, allowing for determining the surface tension.[34]

Besides optical trapping with Gaussian beams described above, trapping aerosol particles with Bessel beams has also been extensively developed.[74] Unlike the Gaussian beam, a Bessel beam can maintain a tight focus with a relatively long length, such as about one centimeter, facilitating the manipulation of the trapped aerosol particle along the beam propagation axis. For the case of transparent or weakly absorbing aerosol particles, the major interaction mechanism between the aerosol particle and the trapping beam is attributed to the gradient and scattering forces. And thus a zeroth-order Bessel beam, where the beam center has a local intensity maximum, is typically applied for such case,[75] as shown in Figure 2(b). Similar to AOT, a single Bessel beam optical trapping also requires the trap laser to propagate upward, so that the scattering force can balance the gravitational force,[76] as depicted by Figure 2(b). The Bessel beam trap can trap particles with size ranging from 1 to 20 μm in diameter,[76] while it requires relatively large laser powers, such as a few tens mW.[77] The technique of Bessel beam trapping typically does not require any microscope objective, and thus it promises more capabilities for coupling with various spectroscopic means. Reid et al. combined a Bessel beam optical trap with continuous wave cavity ring down spectroscopy to measure the extinction cross section of single accumulation mode aerosol particles with radii as small as ~300 nm.[76,78] Signorell et al. pioneered the technique of trapping single aerosol particles with multiple Bessel beams which allows for a more rigid spatial confinement, and they further combined with photoacoustic spectroscopy to study photokinetics and mass accommodation coefficients of aerosols.[79] A combined study of such trapping technique and AOT was also performed to investigate the timescales of water evaporation and condensation in viscous particles down into the submicron size range.[80]

Note that the optical trapping via gradient forces described so far is mostly employed to non-absorbing particles. For the case of strongly absorbing particles, they are manipulated by so-called photophoretic forces instead, which rely on laser heating of the particle. The hot surface of the particle can heat the air molecules hitting this side, and they subsequently rebound with a higher velocity compared to those hitting the cold part of the particle, creating thermal repulsive forces.[28a] Since this photophoretic force is repulsive, particles are confined within the local intensity minimum of the beam, as shown in Figure 2(c). Thus, the laser beam which has a doughnut-shape intensity profile at the beam center, such as hollow beam or vortex beam,[81] could be employed for photophoretic trapping. Furthermore, for a better 3D confinement, the trapping scheme of two counter-propagating beams is typically employed as it can create a so-called optical bottle, where the particle is held in a 3D dark void.[82] The photophoretic forces can be significantly larger than the optical gradient forces described above, while this is at the expense of causing significant heating of the trapped particle.[28a] Shvedov et al. pioneered in utilizing a vortex beam trap to confine and manipulate carbon foam particles of 10–100 μm in size.[81b,83] Pan et al. explored various schemes of hollow beam trapping to manipulate different types of air borne particles, and they further combined photophoretic trapping with Raman spectroscopy or cavity ring-down spectroscopy.[81a,82, 84] Preston et al. combined photophoretic trapping and broadband Mie scattering to determine the sizes of strongly absorbing particles.[38] Finally, Eckerskorn et al. proposed that photophoretic trapping is promising for developing a touch-free system which can precisely position sub-micron bioparticles at the focal spot of an X-ray free electron laser, allowing for significantly improving the efficiency of diffractive imaginings.[85]

As a summary, these recent advances of optical trapping studies demonstrate that combining aerosol optical trapping with various spectroscopic methods allows for probing the structural and dynamical properties of individual aerosol particles and obtaining unprecedented details about the multiphases and heterogeneous dynamics of each single aerosol particle.

2.2. Electrodynamic balance

Besides optical trapping, the other conventional method to trap single aerosol particles is to suspend charged particles inside electric fields. One of famous examples is Millikan's oil drop experiment in 1935 where the charged oil drops were suspended against gravity by means of electrostatic fields, while the lateral movements of oil drops were not confined. In 1953, Good proposed to suspend a charge particle by means of time-varying inhomogeneous electric fields, so that both vertical and lateral movements can be dynamically confined.[86] Such trapping scheme is also called electrodynamic balance (EDB).

The electric fields required by EDB can be generated from linear quadrupole, parallel-plate, ring shape or concentric cylindrical electrodes applied with alternating voltages with radio frequencies.[24d,86b,87] Each design has its own advantages in terms of the trapping stiffness, the open space for optical accesses and the compact size of the trapping chamber.[24a,d,86b] The typical configuration of a linear quadrupole trap which utilizes linear rod electrodes is shown in Figure 6, where the induction electrode is used to charge the particles, and gravitational force on the particle is balanced by the repulsive force provided by the balance electrode with a constant voltage. The EDB devices in modern investigations are usually coupled with an on-demand piezoelectric or thermal driven droplet injector, which can load single droplets only when electric pulses are applied. An advanced piezo-activated droplet generator can produce droplets with specific sizes and velocities by means of tuning the custom voltage waveforms applied to the piezo actuator.[88] The typical sizes of particles in EDB measurements are from few to few tens μm, and they are typically inferred from analyzing the Mie resonances manifested in its elastic light scattering patterns. For more precise measurements of particle sizes, a high-resolution Mie spectroscopy which utilizes a narrow linewidth laser (< 5 MHz) can be employed, and the accuracies for aerosol radius and RI can be within 2 nm and 0.005, respectively.[89] To characterizing the chemistry of the

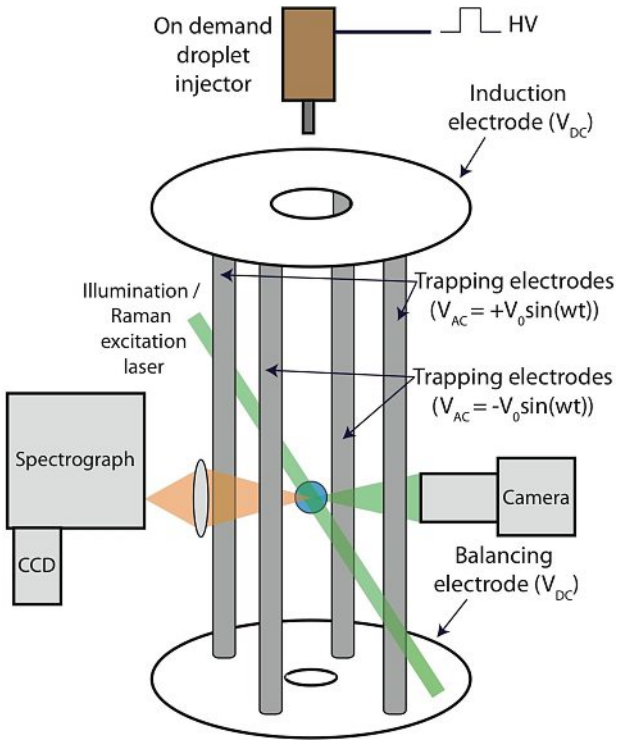

Figure 6. Schematics of linear quadrupole electrodynamic balances, where two pairs of trapping electrodes have opposite phases of alternating voltages. A laser source is guided to hit the trapped aerosol particles, generating elastic and Raman scattering signals, which are detected by a camera and a CCD spectrometer, respectively. The micro-droplets generated from the ink-jet system will be charged after passing through the induction electrode. The gravitation force of the trapped droplet is balanced by the electric field of the balancing electrode.

trapped aerosol particle, the EDB devices are typically coupled with Raman spectroscopy[24d,e] or laser induced fluorescence as nondestructive means to determine chemical compositions and their time evolutions,[90] as shown in Figure 6. However, for the case that more complete information about the chemical compositions is desired due to chemical complexity of atmospheric aerosols, recently some advanced EDB devices were coupled with on-line mass spectrometry, which is in general more sensitive and versatile than conventional optical spectroscopy.[90b,91]

Chan et al. are one of pioneers who utilized EDB to study the chemistry of aerosols.[24e] They combined an EDB and Raman spectroscopy to study gas-particle partitioning, phase transformation and hygroscopicity of various single component and mixed organic/inorganic particles as model atmospheric aerosols.[24e,92] They also coupled the EDB with fluorescence spectroscopy to probe the states of water in aerosols.[93] They also utilized such apparatus to study the changes of chemical compositions of pure oleic acid, linoleic acid and linolenic acid droplets during their ozonolysis.[92k,94]

Krieger et al. utilized EDB combined with broadband or high-resolution Mie spectroscopy to determine water activity, density, refractive index and water diffusivity for aqueous shikimic acid droplets.[89a] Furthermore, they utilize EDB to study the diffusion of CO_2 inside the droplet, and they found that the diffusion coefficients of water and CO_2 can be significantly different in the aerosol particles with high viscosities.[89b] Continetti et al. utilized a mobile EDB coupled with Raman spectroscopy to determine the water diffusion coefficients in single suspended charged sucrose-water and citric acid–water micro-droplets in the 30–60 μm diameter range by means of H_2O/D_2O isotope exchange.[95] They also found that the Stokes-Enistein equation breaks down at high viscosities achieved in the particle phase ($> 10^{12}$ Pa s), agreeing with the literature.[95] Reid et al. developed an EDB consisting of concentric cylindrical electrodes which has advantages of more optical access and a more compact size than conventional EDB.[96] They utilized this EDB to investigate the hygroscopicity, evaporation of volatile components and water transport kinetics from single aqueous organic/inorganic micro-droplets, and these measurements allows for establishing a kinetic model to accurately predict organic aerosol evaporation.[43l,96a,b,97] Recently, this EDB was used to investigate the drying kinetics and particle formation from aerosol droplets in colloidal suspensions.[98] Besides prototype atmospheric aerosols described above, Peng et al. utilized a hyperbolic quadrupole Paul trap to confine single bioparticles, such as viruses and bacterias, as prototype bioaerosols, and they can determine the mass of the charged particles according to their motion patterns inside the trap.[99] Furthermore, Reid et al. utilized this novel approach of EDB to investigate the bioaerosol survival as function of relevant environmental conditions.[100]

Eversole et al. focused on developing a linear electrodynamic quadrupole trap for single levitated particles which has a large optical access and a compact size.[101] Their recent studies focused on developing surface enhanced Raman spectroscopy of single suspended aerosol particles, and the

detection limit of about 10^5 molecules was established for 3–5 μm diameter particles containing about 300 Ag nanoparticles.[102] Recently, Reid et al. combined a linear quadrupole trap and a cavity ring-down spectrometer, and they utilized such apparatus to determine the extinction coefficients and elastic scattering phase functions of spherical and non-spherical inorganic salt particles.[103]

Finally, advanced EDB can even allow for mixing two controlled charged particles and initiating chemical reactions in the mixed particle. Kohno et al. developed a Tandem electrodynamic trap to merge two charged droplets, and then they used Raman spectroscopy to characterize the chemical composition of the mixed particle.[104] As described in *Motivation* section, Wilson et al. have developed a branched quadrupole trap to merge two charged droplets (< 40 μm diameters) with fast mixing times (~400 μs).[90b] They utilized such apparatus to investigate the kinetics of the reaction of o-phthalaldehyde with alanine in the presence of dithiolthreitol. The time revolution of the reaction product was monitored via laser induced fluorescence, and the chemical compositions of droplets before and after mixing were monitored by a paper-spray mass spectrometer.[90b]

3. Emergent Application of Graphene Oxide in Aerosol for Environment

Trapping an aqueous organic compound micro-droplet has become one of the breakthrough techniques to study the reactivity of these compounds at air-water interfaces. As noticed above, PAHs can be stably existing in the environment for a long time, hazardous for the environment and human health. Heterogeneous degradation of PAHs by ozone inside aqueous aerosols remains difficult to study, since PAH micro-droplets are instable for trapping technique, due to the low water solubility and high vapor pressure. Approaches capable of Investigating the PAH-ozone reaction mechanisms in aqueous aerosols directly would bring significant impacts on the goal of establishing a healthier environment.

Graphene oxide (GO) is an oxidized form of 2D characteristic carbon sheet with a single-atom thickness.[105] Compared to pristine graphene materials, the oxygenated functional groups of GO enable the sufficient hydrophilicity to be homogeneously dispersed in aqueous solutions. GO also has both rich contents of aromatic carbon rings and oxygen-functionalized groups, yielding a unique-features acting as surfactant-like PAH. Thus GO is anticipated to stabilized PAH in water aerosols and capable of forming micro-droplets in a range of polar solvent. Thus, aqueous micro-droplet of GO, by combining with the trapping technique, is suitable to mimic and gain a deep understanding of aerosol reaction kinetics with respect to PAH degradation in the presence of ozone oxidant. GO has also emerged as a promising adsorbent for PAH removal from the environment. The abundance of pi-electrons and local hydrophobicity of GO allows PAHs to anchor on the basal plane on GO surface. Even though GO has a shortened, local-area-limited electron conjugation compared to graphene, its surfactant characteristics is greatly useful to investigate aerosol-scale PAHs interaction with ozone in aqueous environmnet.[106]

For this purpose, it is important to understand several key factors that manipulate the surfactant characteristics of GO. First, GO synthesis with varied oxidation degrees, also refer to the amounts of oxygenated groups, is critical in manipulating the aerosol stability and the reaction behaviors. Second, the literature knowledge of the reaction mechanisms between GO and O_3 in bulk water is important reference for the comparison to the new data gained in aerosol conditions.[107]

3.1. Oxidation degrees in graphene oxide

As described before, GO have the sufficient hydrophilicity to be homogeneously dispersed in aqueous solutions, capable of forming micro-droplets in a range of polar solvents. The combination of hexagonal C=C conjugation moiety and oxygenated groups in GO leads to the surfactant functionality. In addition, these groups of epoxy/hydroxyls, carbonyl, and carboxylic acid on GO enable a certain chemical reactivity that is useful to sense chemical changes. As pristine graphene is highly electric conductive, oxidation of graphene opens a band gap for suitable spectroscopic study and applications.[108]

Chemical and spectroscopic properties of GO are highly dependent on the different oxidation degrees manipulated by the synthetic procedure. Studies also confirm that the chemical reactivity of GO in electrochemical catalysis and molecule synthesis are varied with different O/C ratios.[109] For example, highly oxidized GO significantly promotes the synthesis of triazoloquinazolinone compounds with acid sites on both the edge and basal plan of GO.[110] Furthermore, the reaction yield is proportional to the oxidation levels of GO. To gain reasonable reactivity of GO to PAHs and O_3 in a micro-droplet, highly oxidized GO is thus critical.

The Hummers' method,[111] probably the most popular procedure to obtain GO in the past decade, has been able to provide decent O/C ratios (~1.257) in the resultants.[112] To increase the oxidation degrees, Tour group reported to use the greater amounts of oxidants ($KMnO_4$)[113] than the conventional Hummers' method. In addition, the changes of reaction sequence of KMO_4 have also been proved to effectively enlarge the O/C ratios (~1.5).[110] This approach, named as preformed highly acidic oxidizing medium (PAOM), is also capable to oxidize large size graphite crystals into GO, not achievable with the Hummers' method (Figure 7).[112]

3.2. Spectroscopy behaviours of GO for Microdroplet Trapping

Spectroscopy changes that occur in GO when it reacts with other species is critical to trace reaction evolution and kinetics.[114] We focused on discussing the spectroscopy behaviors (i.e. UV-Vis, Raman, and photo-luminance) of GO in the literature, due to the easy adoption of these spectroscopy

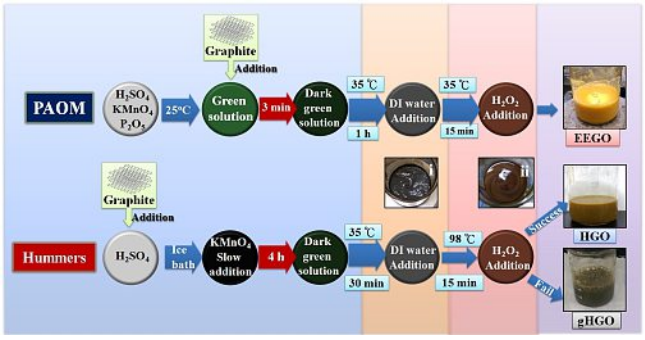

Figure 7. The synthetic procedure of highly acidic oxidizing medium (PAOM) method compare to the Hummers' Method. (Adopted from Ref. [112] with permission. Copyright 2017, Scientific Reports.)

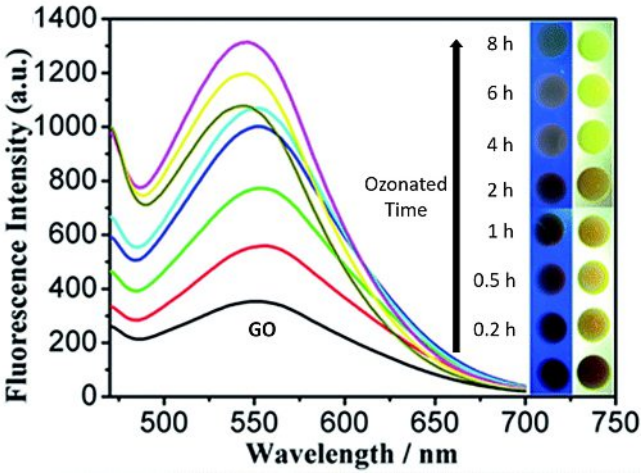

Figure 9. Fluorescence emission of GO (bottom, black) and ozonated-GO over the time from 0.2 h (bottom red curve) to the 8 h ozone exposure. The photographs of the samples, corresponding to the fluorescence spectra with varied ozonation time, under UV lamp (highlighted by the blue-background vertical bar) verses that under white visible light (highlighted by white-background vertical bar), where the exposure time is 0 h, 0.2 h, 0.5 h, 1 h, 2 h, 4 h, 6 h, and 8 h, from bottom to up. (Adopted from Ref. [107b] with permission. Copyright 2014, Royal Society of Chemistry.)

techniques in micro-droplet trapping facility.[107a,b] In the UV-vis spectroscopy, the comparison of GO to ozonated-GO shows a different absorbance peak shifting from 230 nm to 210 nm (Figure 8(a)).[115] The color of GO dispersion changes from deep brown (before) to light yellow, corresponding to the before and after ozonation respectively. The ozonated reaction with GO is interpreted as re-oxidizing GO procedure.[107c,d] This oxidizing procedure breaks down the original pi-electron conjugation in GO and thus the results in the changes in UV-Vis spectroscopy. These data support the possibility of monitoring oxidation reaction and structural changes in GO aerosol for micro-droplet trapping technique.[107a,b]

Raman spectroscopy is also a widely used technique to characterize GO. The D band (~1350 cm^{-1}) to G band (~1580 cm^{-1}) ratios have been reported to estimate the degrees of defects in GO structures (See Figure 8(b)).[115] The higher D/G ratios are considered to be yielding more structure defects. However, some literature also suggests the uncertainty of using Raman to quantify changes of defects. More detailed experiments may be needed to support whether Raman spectroscopy is an effective manner to monitor changes of GO aerosol.[107b,115]

Based on the literature, emission of fluorescence was also used to characterize the changes in GO after ozonation. Yang et al. showed that the fluorescence intensity of GO was significantly alternated after certain time of ozone exposure (Figure 9).[107b] The oxygen groups (e.g. mainly hydroxyls and epoxides) of GO are suggested to be converted into carboxyl and carbonyl groups up to 8 h exposure to ozone, resulting in a re-emission that enhances its fluorescence intensity.[107b] These literatures together suggest that spectroscopy techniques of UV-Vis, Raman, and fluorescence are promising to monitor the chemical changes of GO in AOT operation for the understanding of the reaction mechanisms.

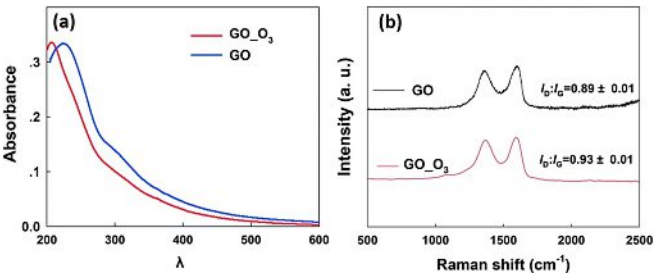

Figure 8. (a) Absorbance data of GO (blue) and Ozonated GO (GO_O_3, red) show a shift to smaller wavelength. (b) Raman spectra of GO ($I_D/I_G = 0.89 \pm 0.01$) and Ozonated GO ($I_D/I_G = 0.93 \pm 0.01$). (Adopted from Ref. [115] with permission. Copyright 2019, Royal Society of Chemistry.)

3.3. Interaction Mechanism between GO and Ozone

The previous studies have revealed that OH radical, formed by ozone-water interaction, is the key species that actively interacts with, or decomposes GO. Pathways involve OH radical are the main concern. One example is that pH values can influence the amounts of OH radical. Ahn et al.[107c] and Yoon et al.[107d] suggest that at high pH, ozone tends to be converted into OH radical, while few radical presents in acidic condition. In a basic condition, OH radical is more reactive and, as a result, GO decomposition should occur more effectively.[115] If this behavior can be quantized, this may suggest the possibility of using GO to determine local pH values of an individual, specific aerosol.

Ozone is an unstable oxidant that readily transforms into another reactive oxygen species in solution.[107c,d,115,116] As noticed earlier, the condition that most influences this ozone decomposition is the pH of the solution.[117] At very acidic condition (pH < 2), ozone does not tend to decompose for OH radical generation. For an acid condition (5 > pH > 2), the reaction pathways are,

$$O_3 + OH^- \rightarrow O_2 \cdot^- + HO_2 \cdot \quad (1)$$

$$O_2 \cdot^- + H^+ \rightarrow HO_2 \rightarrow OH\cdot \quad (2)$$

at neutral condition (pH ~ 7) to basic condition (pH < 14),

$$O_3 + OH^- \rightarrow HO_2^- + O_2 \quad (3)$$

$$O_3 + HO_2^- \rightarrow OH\cdot + O_2 + O_2 \cdot^- \quad (4)$$

And at very basic condition (pH ~ 14),

$$O_3 + OH^- \rightarrow OH\cdot + O_3 \cdot^- \quad (5)$$

Du et al. further verified the decomposition capability of OH radicals on GO. At a constant pH condition, they used the tert-butanol as OH radical scavenger to compare with the GO oxidation efficiency in the presence of OH radical. The results showed that, with the presence of OH radical together with ozone, the oxygenated functional groups on GO will be more actively in oxidization reaction compare to the condition supplying ozone only. Ozone reactivity seems to occur more actively at the edge of GO, rather than on the continuous C=C double bond and/or aromatic rings.[115] In their further study, OH radical interacts with the aromatic rings to produce phenol-like moieties, occurring on both pristine and oxygenated aromatic carbon rings (see a1 and c1 of Figure 10). Ozone alone is not capable of oxidizing unfunctionalized aromatic carbon rings. The ozone can only interact with the OH-activated rings, followed by the aromatic ring cleavage. These results provide a comprehensive background to study the molecular structure changes in GO-ozone interaction in aerosol state using AOT.[115]

4. Challenges and Future Opportunities

Here we discuss several potential challenges and opportunities of exploring the chemistry characteristic of controlled GO aerosol particles. The first challenge is to design a suitable trapping scheme to spatially confine single GO micro-droplets. The UV-Vis absorption spectra of aqueous GO indicate that it has a broad absorptions range, such as from 200 nm to 800 nm (see Figure 8(a)).[115,118] Thus, photophoretic force could be the main mechanism of optically trapping concentrated aqueous GO aerosols with trapping laser wavelengths in the UV-Vis region. Indeed, our preliminary results of our single-beam AOT utilizing a 532 nm cw laser showed that while the concentrated aqueous GO micro-droplets were captured by the laser beam, they were actually trapped at the intensity local minimum of the laser beam spot, as shown in Figure 11(a). Such result indicates that the main trapping mechanism in this case is due to photophoretic force. As there was no GO droplet trapped at the intensity local maximum of the laser beam spot (green spots in Figure 11(a)), which is also the detection region, neither Raman or fluorescence signal of the trapped GO droplets was detected in such trapping configuration. Note that these spatially confined GO micro-droplets shown in Figure 11(a) frequently contacted with each other because of their partially allowed movements in a cyclic path around the beam center, but they exhibited a less tendency to coalesce with each other than typical aqueous droplets, implying the higher surface tensions of these GO droplets. On the other hand, we have also trapped single diluted aqueous GO droplets successfully, and the corresponding bright-field imaging (see the inset of Figure 11(b)) demonstrates that the trapped droplet was three-dimensionally confined at the center of the trapping laser, verifying that the major trapping mechanism in this case is gradient force instead. The observed emission spectrum of the trapped GO droplet (see Figure 11(b)) exhibits not only the Raman signals of water and GO, but also the fluorescence signals of GO, which is similar to the fluorescence spectra of GO in previous works.[118a] The fluorescence intensity of diluted GO droplets in future experiments can be further enhanced by utilizing shorter wavelength excitations,[118a] such as 405 nm for such case. Finally, it is also possible to utilize EDB or the drop-on-demand approach to spatially trap or manipulate concentrated aqueous GO micro-droplets, and these strategies further

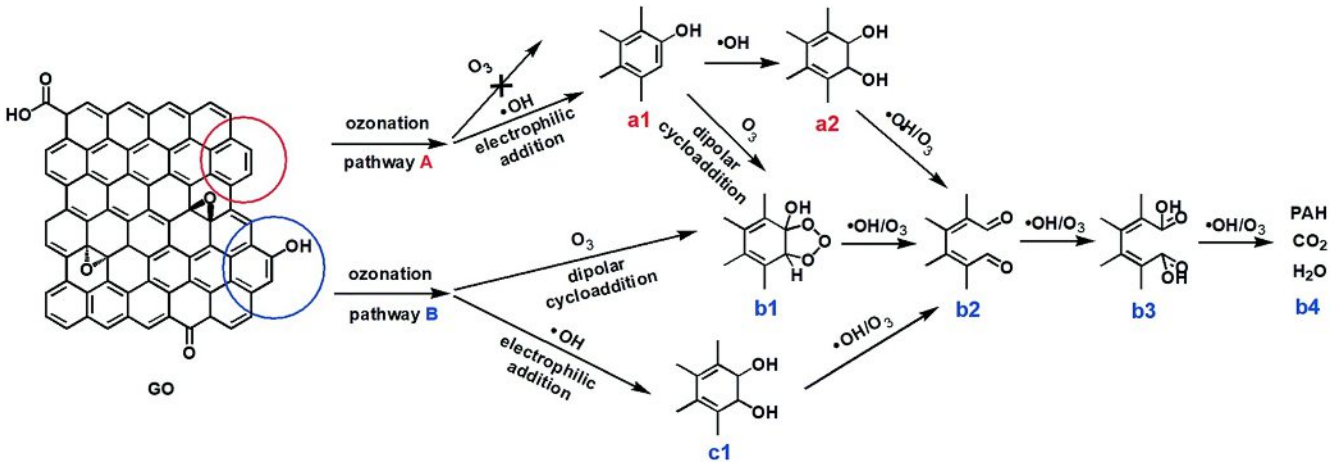

Figure 10. Proposed mechanism Pathway from Du et al. There are two pathways of ozone interaction that is preceded by ozone or OH radical. (Adopted from Ref. [115] with permission. Copyright 2019, Royal Society of Chemistry.)

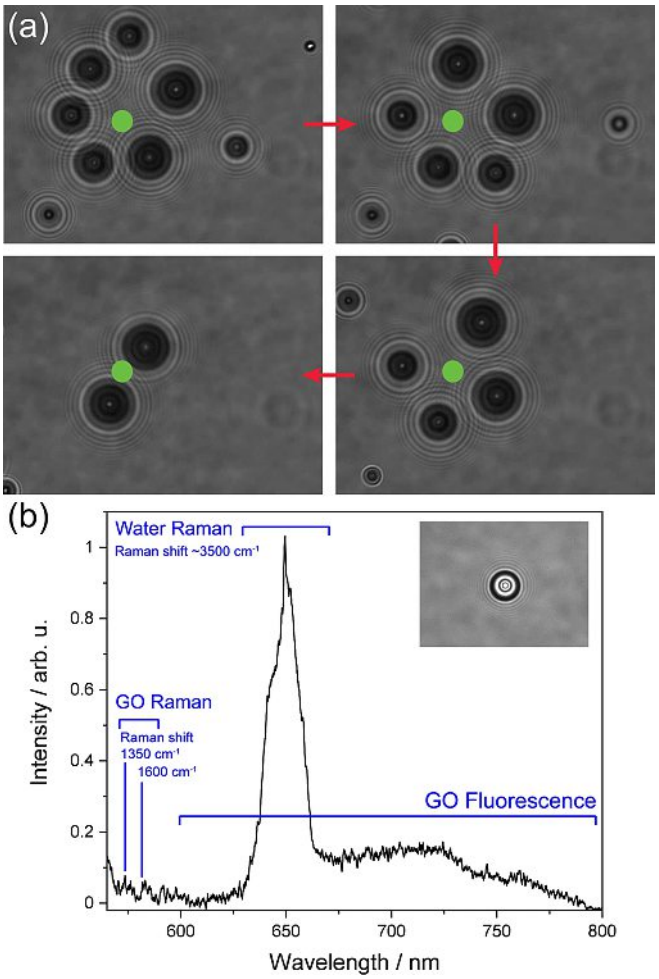

Figure 11. (a) Brightfield imaging of trapped concentrated GO droplets via AOT and the time evolution, measured by this work. Green spots in individual frames represent the center positions of the focused laser beam spots. Red arrows between individual frames indicate the direction of time, and the time durations between adjacent frames are about 30 seconds. (b) Emission spectrum of the diluted aqueous GO droplet. Blue bars represent the tentative assignments. The inset shows the brightfield image of the trapped droplet.

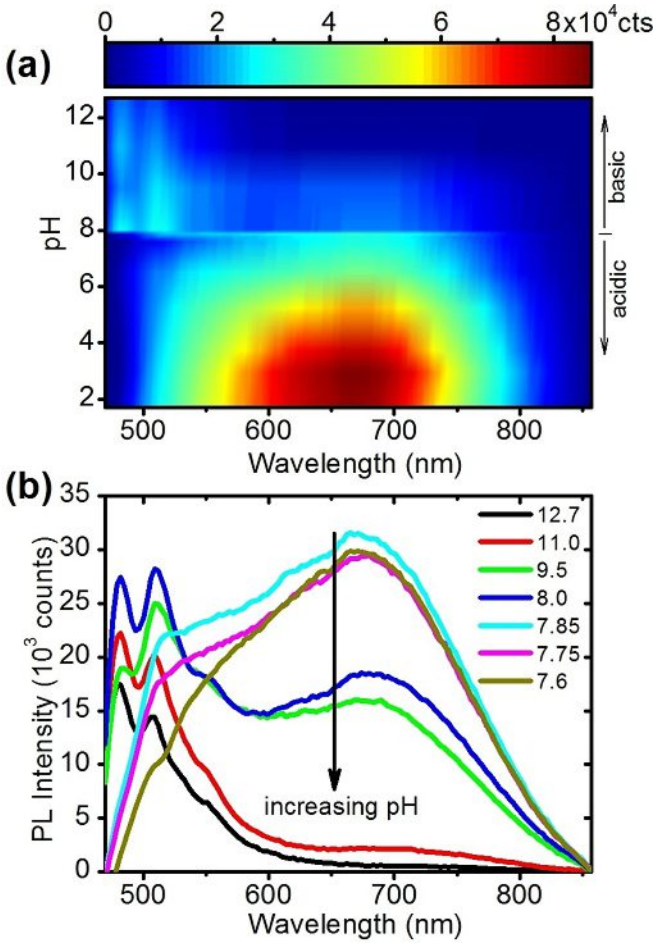

Figure 12. pH dependent fluorescence spectra of GO. (a) Emission spectra measured with 440 nm excitation for sample pH values between 1.7 and 12.7. (b) Traces from Figure 12(a) measured in the basic range from pH 7.6 to 12.7. (Reprinted with permission from Ref. [118b], Copyright 2011 Springer Nature.)

allow for coupling with more spectroscopic tools, such as UV-Vis absorption spectroscopy, and avoiding any limitation due to the spectral range of objective lens typically used for optical trapping and unwanted interaction between the trapping laser field and the target particle.

Spatially-Controlled aqueous GO droplets promise several novel investigations associated with aerosol and environmental chemistry. The first promising application is to use GO as a pH sensor to determine the pH of micro-droplets, which can have play an important role in the formation of atmospheric SOAs and health effects.[51] The previous work of Galande et al.[118b] has demonstrated that the emission spectra of aqueous GO can exhibit a significant pH dependence over a wide range of pH, as shown in Figure 12, and thus aerosol pH can be retrieved from the emission spectra of GO inside droplets. The main advantage of such method is that the fluorescence detection can be more sensitive than Raman detection of pH described before, while the low quantum yield of GO may be a potential issue. This fluorescence detection also has its advantage for knowing changes in a GO aerosol interaction with ozone in a predefined pH. Such strategy could be extended to determine the pH near the air-water interfaces of micro-droplets, when single-molecule detection methods are employed to measure the fluorescence of interfacial GO, which behave as two-dimensional surfactants. Furthermore, combining with fluorescence imaging microscopy will open up an opportunity to map the pH gradient of a whole aerosol particle. Such measurement of the pH gradient inside micro-droplets will provide more insights about the heterogeneous chemistry of biosurfaces where the acidity of interfacial fluids could be a key factor of affecting health effects.[9a,d, 22]

The second promising application is to utilize aqueous GO aerosols as prototype PAH in aerosol phase, allowing for elucidating the heterogeneous chemistry of GO and PAH oxidations. As described in *Motivation* Section, the chemical fates of PAHs in aerosol phase can be significantly affected by the viscosity of SOA and the diffusion rate of PAHs inside SOA. Thus, the proposed kinetics study of the ozonolysis of single trapped aqueous GO aerosols should couple the *in situ*, real-

time and non-destructive measurements of aerosol viscosity or diffusion coefficient, such as fluorescent lifetime of molecular rotors or fluorescence correlation spectroscopy.[60] The reaction kinetics and mechanism can also be different in bulk solution than in aerosol because several intermediates could exist longer/shorter in time at the aerosol phase. Only such combined investigation of single aerosol particle spectroscopy can further elucidate the interplay between aerosol viscosity and formation rate of GO SOA. It is also necessary to characterize the compositions of reaction products by means of on-line mass spectrometry which can have higher sensitivities of PAHs than optical spectroscopy, in order to clarify the reaction pathways and to quantify their contribution to the viscosity of aging aerosols. Coupling the single particle traps to on-line mass spectrometry is still a challenging task, while there have been several successful demonstrations.[25b,90b,91] One key issue of such application is the efficient desorption/ionization of the species of interest inside each aerosol particle. Besides the paper spray ionization, field-induced ionization and the combination of thermal vaporization and corona discharge which have been demonstrated with single particle traps,[25b,90b,91] several advanced methods dedicated to single particle ionization, such as droplet electrospray via charged needle and laser desorption/ionization,[119] promise the feasibility of single particle mass spectrometers coupled with single particle traps.

Finally, we will explore the possibilities of utilizing aqueous GO droplets to remove hazardous PAHs from gaseous environments via π-π interactions between GO and PAHs.[120] In aerosol phase, most aqueous GO will be enriched near the air-water interface, increasing the contacted surface area and efficiency of absorbing gaseous PAHs via interfacial GO. In the previous research, Wang et al. proposed that H-π and anion-π interaction may occur between the oxygen-functionalized GO and the aromatic rings from PAH. Zhang et al. discovered a unique adsorption behavior of brilliant blue (BB) on GO, allowing BB to be stably dispersed in water. GO is also shown to be a promising adsorbent for PAHs including anthracenemethanol and fluoranthene.[121] With these examples of proving PAH to GO interfacial interaction, the GO aerosol-spray method can be a promising, simplified strategy for PAH-removal, as this does not require any preparation of GO film or other pre-synthesis. The proposed investigation of single aerosol spectroscopy coupled with aerosol trapping here will allow for elucidating the interaction mechanism of interfacial GO and PAHs and the dependences to various properties of GO droplets, such as aerosol pH, GO droplet size, and functional groups of GO.

5. Conclusion

Optical trapping and electrodynamic balance provide means to control the motion of single micro-droplets. Coupling these trapping methods with optical spectroscopy means can facilitate various novel investigations of single particle spectroscopy, allowing for the *in situ* and real time determination of physicochemical properties each single aerosol particle, such as particle radius, temperature, phase, pH, viscosity, diffusion rate, surface tension, chemical compositions, solute strength and reaction rate, as well as their inhomogeneities in aerosol phase. Only such detailed investigation allows for elucidating the delicate interplays among these physicochemical properties of single aerosol particle during its dynamical processes. In this review we described several well-established experimental schemes for trapping various kinds of aerosol particles, and we also introduced their novel applications of coupling with various advanced optical spectroscopy to measure those physicochemical properties of single trapped aerosol particles. We also described several recent breakthroughs which exploited such approach of single-particle trapping and detection to study various dynamical processes of prototypical atmospheric aerosols, aiming to resolve several key issues in atmospheric chemistry.

Because of unique chemical and physical properties of GO, in this review we introduce the promising potentials of GO micro-droplets as prototype PAH aerosols. The heterogeneous chemistry of atmospheric PAHs in aerosol phase is still a key issue associated with atmospheric chemistry and human health, while the bulk measurements could only provide limited information. The investigation of aqueous GO aerosol ozonolysis by means of single aerosol trapping and detection will provide key insights about the reaction mechanism and kinetics of the chemical degradation of PAH aerosols in unprecedented details. We also detailed the other potential applications of spatially-controlled aqueous GO aerosols, such as interfacial pH sensor or atmospheric PAH scavenger, which we rationalize the feasibility with the current state of the art. We believe that the experiments described in this article are an important step forward to a healthier environment, and such step is supported by comprehensive understanding of aerosol chemistry and innovations of aerosol technology.

Acknowledgements

This work was supported by the Ministry of Science and Technology, Taiwan (MOST107-2113-M-110-004-MY3 and MOST109-2113-M-110-010-). We thank Ms. Feng-Yu Lin and Ms. Jia-Rong Li for the preliminary data of GO aerosol trapping via AOT, and Ms. Shan-Jung Wu and Mr. Che-Yu Chiang for AOT data of citric acid and ascorbic acid.

Conflict of Interest

The authors declare no conflict of interest.

Keywords: Aerosol · Graphene oxide · Raman spectroscopy · Optical tweezers · Ozonolysis · Polycyclic aromatic hydrocarbons

[1] a) U. Poschl, *Angew. Chem. Int. Ed.* **2005**, *44*, 7520–7540; *Angew. Chem.* **2005**, *117*, 7690–7712; b) A. P. Ault, J. L. Axson, *Anal. Chem.* **2017**, *89*, 430–452.

[2] a) S. Zhou, M. Shiraiwa, R. D. McWhinney, U. Poschl, J. P. Abbatt, *Faraday Discuss.* **2013**, *165*, 391–406; b) J. P. Reid, A. K. Bertram, D. O. Topping, A. Laskin, S. T. Martin, M. D. Petters, F. D. Pope, G. Rovelli, *Nat. Commun.* **2018**, *9*, 956.
[3] a) K. J. Laidler, *Chemical Kinetics*, Harper Collins Inc., **1987**; b) M. Mekic, M. Brigante, D. Vione, S. Gligorovski, *Atmos. Environ.* **2018**, *185*, 237–242; c) M. Mekic, Y. Wang, G. Loisel, D. Vione, S. Gligorovski, *Environ. Sci. Technol.* **2020**, *54*, 12898–12907.
[4] T. Liu, S. L. Clegg, J. P. D. Abbatt, *Proc. Natl. Acad. Sci. USA* **2020**, *117*, 1354–1359.
[5] J. P. Reid, R. M. Sayer, *Chem. Soc. Rev.* **2003**, *32*, 70–79.
[6] a) M. T. C. Martins-Costa, J. M. Anglada, J. S. Francisco, M. F. Ruiz-Lopez, *Angew. Chem. Int. Ed.* **2012**, *51*, 5413–5417; *Angew. Chem.* **2012**, *124*, 5509–5513; b) M. T. C. Martins-Costa, J. M. Anglada, J. S. Francisco, M. F. Ruiz-Lopez, *J. Am. Chem. Soc.* **2012**, *134*, 11821–11827.
[7] a) M. A. Brown, B. Winter, M. Faubel, J. C. Hemminger, *J. Am. Chem. Soc.* **2009**, *131*, 8354–8355; b) D. E. Otten, R. Onorato, R. Michaels, J. Goodknight, R. J. Saykally, *Chem. Phys. Lett.* **2012**, *519–520*, 45–48; c) C.-C. Su, Y. Yu, P.-C. Chang, Y.-W. Chen, I.-Y. Chen, Y.-Y. Lee, C. C. Wang, *J. Phys. Chem. Lett.* **2015**, *6*, 817–823; d) P.-C. Lin, Z.-H. Wu, M.-S. Chen, Y.-L. Li, W.-R. Chen, T.-P. Huang, Y.-Y. Lee, C. C. Wang, *J. Phys. Chem. B* **2017**, *121*, 1054–1067.
[8] P.-C. Chang, Y. Yu, Z.-H. Wu, P.-C. Lin, W.-R. Chen, C.-C. Su, M.-S. Chen, Y.-L. Li, T.-P. Huang, Y.-Y. Lee, C. C. Wang, *J. Phys. Chem. B* **2016**, *120*, 10181–10191.
[9] a) S. Enami, M. R. Hoffmann, A. J. Colussi, *Proc. Natl. Acad. Sci. USA* **2008**, *105*, 7365–7369; b) S. Enami, A. J. Colussi, *J. Phys. Chem. Lett.* **2017**, *8*, 1615–1623; c) S. Enami, M. R. Hoffmann, A. J. Colussi, *J. Phys. Chem. Lett.* **2017**, *8*, 3888–3894; d) S. Enami, M. R. Hoffmann, A. J. Colussi, *J. Phys. Chem. B* **2008**, *112*, 4153–4156.
[10] a) X. Yan, R. M. Bain, R. G. Cooks, *Angew. Chem. Int. Ed.* **2016**, *55*, 12960–12972; *Angew. Chem.* **2016**, *128*, 13152–13166; b) M. Girod, E. Moyano, D. I. Campbell, R. G. Cooks, *Chem. Sci.* **2011**, *2*, 501–510; c) A. Fallah-Araghi, K. Meguellati, J.-C. Baret, A. E. Harrak, T. Mangeat, M. Karplus, S. Ladame, C. M. Marques, A. D. Griffiths, *Phys. Rev. Lett.* **2014**, *112*, 028301; d) T. Müller, A. Badu-Tawiah, R. G. Cooks, *Angew. Chem. Int. Ed.* **2012**, *51*, 11832–11835; *Angew. Chem.* **2012**, *124*, 12002–12005; e) Z. Wei, Y. Li, R. G. Cooks, X. Yan, *Annu. Rev. Phys. Chem.* **2020**, *71*, 31–51.
[11] a) E. T. Jansson, Y.-H. Lai, J. G. Santiago, R. N. Zare, *J. Am. Chem. Soc.* **2017**, *139*, 6851–6854; b) I. Nam, J. K. Lee, H. G. Nam, R. N. Zare, *Proc. Natl. Acad. Sci. USA* **2017**, *114*, 12396–12400; c) I. Nam, H. G. Nam, R. N. Zare, *Proc. Natl. Acad. Sci. USA* **2018**, *115*, 36–40; d) K. L. Walker, L. M. Dornan, R. N. Zare, R. M. Waymouth, M. J. Muldoon, *J. Am. Chem. Soc.* **2017**, *139*, 12495–12503; e) J. K. Lee, D. Samanta, H. G. Nam, R. N. Zare, *Nat. Commun.* **2018**, *9*, 1562.
[12] R. M. Bain, S. Sathyamoorthi, R. N. Zare, *Angew. Chem. Int. Ed.* **2017**, *129*, 15279–15283.
[13] J. K. Lee, K. L. Walker, H. S. Han, J. Kang, F. B. Prinz, R. M. Waymouth, H. G. Nam, R. N. Zare, *Proc. Natl. Acad. Sci. USA* **2019**, *116*, 19294–19298.
[14] J. K. Lee, D. Samanta, H. G. Nam, R. N. Zare, *J. Am. Chem. Soc.* **2019**, *141*, 10585–10589.
[15] a) E. K. Athanassiou, R. N. Grass, W. J. Stark, *Aerosol Sci. Technol.* **2010**, *44*, 161–172; b) S. H. Kim, B. Y. H. Liu, M. R. Zachariah, *Chem. Mater.* **2002**, *14*, 2889–2899; c) M. L. Eggersdorfer, S. E. Pratsinis, *Adv. Powder Technol.* **2014**, *25*, 71–90; d) M. Woźniak, J. Archer, T. Wojciechowski, G. Derkachov, T. Jakubczyk, K. Kolwas, M. Kolwas, D. Jakubczyk, *J. Instrum.* **2019**, *14*, P12007–P12007; e) Z. Long, Y. Wang, Q. Fu, J. Ouyang, L. He, N. Na, *Nanoscale* **2019**, *11*, 11093–11098; f) Y. Chen, F. Guo, A. Jachak, S.-P. Kim, D. Datta, J. Liu, I. Kulaots, C. Vaslet, H. D. Jang, J. Huang, A. Kane, V. B. Shenoy, R. H. Hurt, *Nano Lett.* **2012**, *12*, 1996–2002; g) X. Ma, M. R. Zachariah, C. D. Zangmeister, *Nano Lett.* **2012**, *12*, 486–489; h) E. Jabari, E. Toyserkani, *Carbon* **2015**, *91*, 321–329; i) Y. Jiang, W.-N. Wang, P. Biswas, J. D. Fortner, *ACS Appl. Mater. Interfaces* **2014**, *6*, 11766–11774.
[16] S.-Y. Hsu, S.-C. Lin, J.-A. Wang, C.-C. Hu, C.-C. M. Ma, D.-H. Tsai, *Electrochim. Acta* **2019**, *296*, 427–437.
[17] T. Cheng, J. Xu, Z. Tan, J. Ye, Z. Tao, Z. Du, Y. Wu, S. Wu, H. Ji, Y. Yu, Y. Zhu, *Energy Storage Mater.* **2018**, *10*, 282–290.
[18] M. Wozniak, G. Derkachov, K. Kolwas, J. Archer, T. Wojciechowski, D. Jakubczyk, M. Kolwas, *Langmuir* **2015**, *31*, 7860–7868.
[19] B. J. Finlayson-Pitts, J. N. Pitts, Jr., *Science* **1997**, *276*, 1045–1052.
[20] S. Zhou, B. C. H. Hwang, P. S. J. Lakey, A. Zuend, J. P. D. Abbatt, M. Shiraiwa, *Proc. Natl. Acad. Sci. USA* **2019**, *116*, 11658–11663.
[21] M. Shrivastava, S. Lou, A. Zelenyuk, R. C. Easter, R. A. Corley, B. D. Thrall, P. J. Rasch, J. D. Fast, S. L. Massey Simonich, H. Shen, S. Tao, *Proc. Natl. Acad. Sci. USA* **2017**, *114*, 1246–1251.
[22] Y. P. Chang, S. J. Wu, M. S. Lin, C. Y. Chiang, G. G. Huang, *Phys. Chem. Chem. Phys.* **2021**, *23*, 10108–10117.
[23] a) H. Suzuki, Y. Matsuzaki, A. Muraoka, M. Tachikawa, *J. Chem. Phys.* **2012**, *136*, 234508; b) A. Miura, R. Nakajima, S. Abe, N. Kitamura, *J. Phys. Chem. A* **2020**, *124*, 9035–9043; c) S. Ishizaka, T. Wada, N. Kitamura, *Chem. Phys. Lett.* **2011**, *506*, 117–121.
[24] a) U. K. Krieger, C. Marcolli, J. P. Reid, *Chem. Soc. Rev.* **2012**, *41*, 6631; b) J. P. Reid, *J. Quant. Spectrosc. Radiat. Transfer* **2009**, *110*, 1293–1306; c) G. Schweiger, *J. Aerosol Sci.* **1990**, *21*, 483–509; d) E. J. Davis, *Aerosol Sci. Technol.* **1997**, *26*, 212–254; e) A. Lee, C. Chan, in *Fundamentals and Applications in Aerosol Spectroscopy* (Eds.: R. Signorell, J. Reid), CRC Press, **2011**, pp. 155–191; f) R. M. Power, J. P. Reid, *Rep. Prog. Phys.* **2014**, *77*, 074601; g) A. Marsh, G. Rovelli, Y.-C. Song, K. L. Pereira, R. E. Willoughby, B. R. Bzdek, J. F. Hamilton, A. J. Orr-Ewing, D. O. Topping, J. P. Reid, *Faraday Discuss.* **2017**, *200*, 639–661; h) L. Mitchem, J. P. Reid, *Chem. Soc. Rev.* **2008**, *37*, 756; i) J. B. Wills, K. J. Knox, J. P. Reid, *Chem. Phys. Lett.* **2009**, *481*, 153–165; j) R. E. H. Miles, A. E. Carruthers, J. P. Reid, *Laser Photonics Rev.* **2011**, *5*, 534–552.
[25] a) N. J. Mason, E. A. Drage, S. M. Webb, A. Dawes, R. McPheat, G. Hayes, *Faraday Discuss.* **2008**, *137*, 367–376; discussion 403–324; b) C. Mu, J. Wang, K. M. Barraza, X. Zhang, J. L. Beauchamp, *Angew. Chem. Int. Ed.* **2019**, *58*, 8082–8086; *Angew. Chem.* **2019**, *131*, 8166–8170.
[26] a) A. R. Metcalf, S. Narayan, C. S. Dutcher, *Aerosol Sci. Technol.* **2017**, *52*, 310–329; b) L. Nandy, C. S. Dutcher, *J. Phys. Chem. B* **2018**, *122*, 3480–3490; c) P. Roy, S. Liu, C. S. Dutcher, *Annu. Rev. Phys. Chem.* **2021**, *72*, 73–97; d) S. Narayan, D. B. Moravec, A. J. Dallas, C. S. Dutcher, *Physical Review Fluids* **2020**, *5*, 113603; e) A. R. Metcalf, H. C. Boyer, C. S. Dutcher, *Environ. Sci. Technol.* **2016**, *50*, 1251–1259.
[27] A. Ashkin, J. M. Dziedzic, J. E. Bjorkholm, S. Chu, *Opt. Lett.* **1986**, *11*, 288.
[28] a) R. W. Bowman, M. J. Padgett, *Rep. Prog. Phys.* **2013**, *76*, 026401; b) A. Ashkin, J. Dziedzic, *Science* **1987**, *235*, 1517–1520.
[29] a) A. Ashkin, J. M. Dziedzic, *Science* **1975**, *187*, 1073–1075; b) R. Omori, T. Kobayashi, A. Suzuki, *Opt. Lett.* **1997**, *22*, 816–818; c) M. D. Summers, D. R. Burnham, D. McGloin, *Opt. Express* **2008**, *16*, 7739–7747; d) A. Ashkin, J. M. Dziedzic, *Appl. Phys. Lett.* **1971**, *19*, 283–285; e) N. Magome, M. I. Kohira, E. Hayata, S. Mukai, K. Yoshikawa, *J. Phys. Chem. B* **2003**, *107*, 3988–3990; f) G. G. Hoffmann, E. Lentz, B. Schrader, *Rev. Sci. Instrum.* **1993**, *64*, 823–824.
[30] D. R. Burnham, D. McGloin, *J. Opt. Soc. Am. B* **2011**, *28*, 2856.
[31] R. J. Hopkins, L. Mitchem, A. D. Ward, J. P. Reid, *Phys. Chem. Chem. Phys.* **2004**, *6*, 4924.
[32] M. D. King, K. C. Thompson, A. D. Ward, *J. Am. Chem. Soc.* **2004**, *126*, 16710–16711.
[33] a) K. J. Knox, *Light-Induced Processes in Optically-Tweezed Aerosol Droplets*, Springer Berlin Heidelberg, Berlin, Heidelberg, **2011**; b) K. J. Knox, J. P. Reid, K. L. Hanford, A. J. Hudson, L. Mitchem, *J. Opt. A* **2007**, *9*, S180–S188.
[34] A. Rafferty, K. Gorkowski, A. Zuend, T. C. Preston, *Proc. Natl. Acad. Sci. USA* **2019**, *116*, 19880–19886.
[35] a) A. Rafferty, T. C. Preston, *Phys. Chem. Chem. Phys.* **2018**, *20*, 17038–17047; b) S. H. Jones, M. D. King, A. D. Ward, *Phys. Chem. Chem. Phys.* **2013**, *15*, 20735–20741.
[36] a) L. Rkiouak, M. J. Tang, J. C. J. Camp, J. McGregor, I. M. Watson, R. A. Cox, M. Kalberer, A. D. Ward, F. D. Pope, *Phys. Chem. Chem. Phys.* **2014**, *16*, 11426–11434; b) H. J. Tong, C. Fitzgerald, P. J. Gallimore, M. Kalberer, M. K. Kuimova, P. C. Seville, A. D. Ward, F. D. Pope, *Chem. Commun.* **2014**, *50*, 15499–15502; c) P. J. Gallimore, N. M. Davidson, M. Kalberer, F. D. Pope, A. D. Ward, *Anal. Chem.* **2018**, *90*, 8838–8844.
[37] L. Mitchem, J. Buajarern, R. J. Hopkins, A. D. Ward, R. J. J. Gilham, R. L. Johnston, J. P. Reid, *J. Phys. Chem. A* **2006**, *110*, 8116–8125.
[38] a) N.-O. A. Kwamena, J. P. Reid, in *Fundamentals and Applications in Aerosol Spectroscopy*, 0 ed. (Eds.: R. Signorell, J. P. Reid), CRC Press, **2010**, pp. 146–173; b) J. P. Reid, L. Mitchem, *Annu. Rev. Phys. Chem.* **2006**, *57*, 245–271.
[39] a) T. C. Preston, J. P. Reid, *J. Opt. Soc. Am. B* **2013**, *30*, 2113; b) T. C. Preston, J. P. Reid, *J. Opt. Soc. Am. A* **2015**, *32*, 2210; c) J. P. Reid, H. Meresman, L. Mitchem, R. Symes, *Int. Rev. Phys. Chem.* **2007**, *26*, 139–192; d) R. Symes, R. M. Sayer, J. P. Reid, *Phys. Chem. Chem. Phys.* **2004**, *6*, 474–487; e) G. Hargreaves, N. O. A. Kwamena, Y. H. Zhang, J. R. Butler, S. Rushworth, S. L. Clegg, J. P. Reid, *J. Phys. Chem. A* **2010**, *114*, 1806–1815; f) R. E. Miles, J. S. Walker, D. R. Burnham, J. P. Reid, *Phys.*

Chem. Chem. Phys. **2012**, *14*, 3037–3047; g) K. J. Knox, J. P. Reid, *J. Phys. Chem. A* **2008**, *112*, 10439–10441.
[40] A. E. Haddrell, R. E. H. Miles, B. R. Bzdek, J. P. Reid, R. J. Hopkins, J. S. Walker, *Anal. Chem.* **2017**, *89*, 2345–2352.
[41] R. E. H. Miles, K. J. Knox, J. P. Reid, A. M. C. Laurain, L. Mitchem, *Phys. Rev. Lett.* **2010**, *105*, 116101.
[42] J. Buajarern, L. Mitchem, A. D. Ward, N. H. Nahler, D. McGloin, J. P. Reid, *J. Chem. Phys.* **2006**, *125*, 114506.
[43] a) C. Cai, D. J. Stewart, T. C. Preston, J. S. Walker, Y.-H. Zhang, J. P. Reid, *Phys. Chem. Chem. Phys.* **2014**, *16*, 3162; b) C. Cai, C. Zhao, *Atmos. Environ.* **2018**, *189*, 50–60; c) X.-J. Lv, Y. Wang, C. Cai, S.-F. Pang, J.-B. Ma, Y.-H. Zhang, *Spectrochim. Acta Part A* **2018**, *200*, 179–185; d) B. J. Dennis-Smither, K. L. Hanford, N.-O. A. Kwamena, R. E. H. Miles, J. P. Reid, *J. Phys. Chem. A* **2012**, *116*, 6159–6168; e) B. J. Dennis-Smither, F. H. Marshall, R. E. H. Miles, T. C. Preston, J. P. Reid, *J. Phys. Chem. A* **2014**, *118*, 5680–5691; f) A. M. J. Rickards, R. E. H. Miles, J. F. Davies, F. H. Marshall, J. P. Reid, *J. Phys. Chem. A* **2013**, *117*, 14120–14131; g) X. J. Lv, Z. Chen, J. B. Ma, Y. H. Zhang, *Spectrochim. Acta Part A* **2020**, *226*, 117552; h) C. Cai, D. J. Stewart, J. P. Reid, Y. H. Zhang, P. Ohm, C. S. Dutcher, S. L. Clegg, *J. Phys. Chem. A.* **2015**, *119*, 704–718; i) D. M. Lienhard, D. L. Bones, A. Zuend, U. K. Krieger, J. P. Reid, T. Peter, *J. Phys. Chem. A* **2012**, *116*, 9954–9968; j) K. L. Hanford, L. Mitchem, J. P. Reid, S. L. Clegg, D. O. Topping, G. B. McFiggans, *J. Phys. Chem. A* **2008**, *112*, 9413–9422; k) J. R. Butler, L. Mitchem, K. L. Hanford, L. Treuel, J. P. Reid, *Faraday Discuss.* **2008**, *137*, 351–366; discussion 403–324; l) F. D. Pope, H.-J. Tong, B. J. Dennis-Smither, P. T. Griffiths, S. L. Clegg, J. P. Reid, R. A. Cox, *J. Phys. Chem. A* **2010**, *114*, 10156–10165; m) L. N. Wang, C. Cai, Y. H. Zhang, *J. Phys. Chem. B* **2017**, *121*, 8551–8557.
[44] a) D. J. Stewart, C. Cai, J. Nayler, T. C. Preston, J. P. Reid, U. K. Krieger, C. Marcolli, Y. H. Zhang, *J. Phys. Chem. A.* **2015**, *119*, 4177–4190; b) J. P. Reid, B. J. Dennis-Smither, N.-O. A. Kwamena, R. E. H. Miles, K. L. Hanford, C. J. Homer, *Phys. Chem. Chem. Phys.* **2011**, *13*, 15559–15572; c) N. O. A. Kwamena, J. Buajarern, J. P. Reid, *J. Phys. Chem. A* **2010**, *114*, 5787–5795; d) J. Buajarern, L. Mitchem, J. P. Reid, *J. Phys. Chem. A* **2007**, *111*, 9054–9061; e) L. Mitchem, J. Buajarern, A. D. Ward, J. P. Reid, *J. Phys. Chem. B* **2006**, *110*, 13700–13703.
[45] a) B. Vennes, T. C. Preston, *J. Opt. Soc. Am. A* **2019**, *36*, 2089–2103; b) A. Moridnejad, T. C. Preston, U. K. Krieger, *J. Phys. Chem. A* **2017**, *121*, 8176–8184; c) J. Buajarern, L. Mitchem, J. P. Reid, *J. Phys. Chem. A* **2007**, *111*, 11852–11859; d) K. Gorkowski, N. M. Donahue, R. C. Sullivan, *Environ. Sci. Technol.* **2017**, *51*, 12154–12163.
[46] a) L. J. N. Lew, M. V. Ting, T. C. Preston, *Appl. Opt.* **2018**, *57*, 4601; b) A. D. Ward, M. Zhang, O. Hunt, *Opt. Express* **2008**, *16*, 16390–16403; c) L. J. Moore, M. D. Summers, G. A. D. Ritchie, *Phys. Chem. Chem. Phys.* **2013**, *15*, 13489–13498.
[47] a) M. D. King, K. C. Thompson, A. D. Ward, C. Pfrang, B. R. Hughes, *Faraday Discuss.* **2008**, *137*, 173–192; b) B. J. Dennis-Smither, R. E. H. Miles, J. P. Reid, *J. Geophys. Res.* **2012**, *117*; c) O. R. Hunt, A. D. Ward, M. D. King, *Phys. Chem. Chem. Phys.* **2015**, *17*, 2734–2741; d) F. H. Marshall, T. Berkemeier, M. Shiraiwa, L. Nandy, P. B. Ohm, C. S. Dutcher, J. P. Reid, *Phys. Chem. Chem. Phys.* **2018**, *20*, 15560–15573.
[48] a) K. Gorkowski, H. Beydoun, M. Aboff, J. S. Walker, J. P. Reid, R. C. Sullivan, *Aerosol Sci. Technol.* **2016**, *50*, 1327–1341; b) R. C. Sullivan, H. Boyer-Chelmo, K. Gorkowski, H. Beydoun, *Acc. Chem. Res.* **2020**, *53*, 2498–2509; c) S. H. Jones, M. D. King, A. D. Ward, *Chem. Commun.* **2015**, *51*, 4914–4917.
[49] J. F. Davies, R. E. H. Miles, A. E. Haddrell, J. P. Reid, *Proc. Natl. Acad. Sci. USA* **2013**, *110*, 8807–8812.
[50] a) J. A. Gomez Castano, L. Boussekey, J. P. Verwaerde, M. Moreau, Y. A. Tobon, *Molecules* **2019**, *24*; b) S. Seng, F. Guo, Y. A. Tobon, T. Ishikawa, M. Moreau, S. Ishizaka, S. Sobanska, *Atmos. Environ.* **2018**, *183*, 33–39.
[51] J. H. Kroll, J. H. Seinfeld, *Atmos. Environ.* **2008**, *42*, 3593–3624.
[52] A. P. Ault, *Acc. Chem. Res.* **2020**, *53*, 1703–1714.
[53] R. L. Craig, L. Nandy, J. L. Axson, C. S. Dutcher, A. P. Ault, *J. Phys. Chem. A* **2017**, *121*, 5690–5699.
[54] a) E. M. Coddens, K. J. Angle, V. H. Grassian, *J. Phys. Chem. Lett.* **2019**, *10*, 4476–4483; b) H. C. Boyer, K. Gorkowski, R. C. Sullivan, *Anal. Chem.* **2020**, *92*, 1089–1096.
[55] a) J. D. Rindelaub, R. L. Craig, L. Nandy, A. L. Bondy, C. S. Dutcher, P. B. Shepson, A. P. Ault, *J. Phys. Chem. A.* **2016**, *120*, 911–917; b) R. L. Craig, P. K. Peterson, L. Nandy, Z. Lei, M. A. Hossain, S. Camarena, R. A. Dodson, R. D. Cook, C. S. Dutcher, A. P. Ault, *Anal. Chem.* **2018**, *90*, 11232–11239.
[56] S.-J. Wu, Master thesis, National Sun Yat-sen University **2021**.
[57] a) G. D. Smith, E. Woods, C. L. DeForest, T. Baer, R. E. Miller, *J. Phys. Chem. A* **2002**, *106*, 8085–8095; b) G. D. Smith, E. Woods, T. Baer, R. E. Miller, *J. Phys. Chem. A* **2003**, *107*, 9582–9587.
[58] a) D. R. Burnham, D. McGloin, *Opt. Express* **2006**, *14*, 4175–4181; b) G. Rovelli, Y.-C. Song, A. M. Maclean, D. O. Topping, A. K. Bertram, J. P. Reid, *Anal. Chem.* **2019**, *91*, 5074–5082; c) B. R. Bzdek, L. Collard, J. E. Sprittles, A. J. Hudson, J. P. Reid, *J. Chem. Phys.* **2016**, *145*, 054502; d) D. McGloin, D. R. Burnham, M. D. Summers, D. Rudd, N. Dewar, S. Anand, *Faraday Discuss.* **2008**, *137*, 335–350; discussion 403–324; e) J. R. Butler, J. B. Wills, L. Mitchem, D. R. Burnham, D. McGloin, J. P. Reid, *Lab Chip* **2009**, *9*, 521–528.
[59] a) Y. C. Song, A. E. Haddrell, B. R. Bzdek, J. P. Reid, T. Bannan, D. O. Topping, C. Percival, C. Cai, *J. Phys. Chem. A* **2016**, *120*, 8123–8137; b) R. M. Power, S. H. Simpson, J. P. Reid, A. J. Hudson, *Chem. Sci.* **2013**, *4*, 2597–2604; c) B. R. Bzdek, R. M. Power, S. H. Simpson, J. P. Reid, C. P. Royall, *Chem. Sci.* **2016**, *7*, 274–285; d) A. Marsh, S. S. Petters, N. E. Rothfuss, G. Rovelli, Y. C. Song, J. P. Reid, M. D. Petters, *Phys. Chem. Chem. Phys.* **2018**, *20*, 15086–15097.
[60] C. Fitzgerald, N. A. Hosny, H. Tong, P. C. Seville, P. J. Gallimore, N. M. Davidson, A. Athanasiadis, S. W. Botchway, A. D. Ward, M. Kalberer, M. K. Kuimova, F. D. Pope, *Phys. Chem. Chem. Phys.* **2016**, *18*, 21710–21719.
[61] A. Athanasiadis, C. Fitzgerald, N. M. Davidson, C. Giorio, S. W. Botchway, A. D. Ward, M. Kalberer, F. D. Pope, M. K. Kuimova, *Phys. Chem. Chem. Phys.* **2016**, *18*, 30385–30393.
[62] F. H. Marshall, R. E. H. Miles, Y. C. Song, P. B. Ohm, R. M. Power, J. P. Reid, C. S. Dutcher, *Chem. Sci.* **2016**, *7*, 1298–1308.
[63] Y.-C. Song, S. Ingram, R. E. Arbon, D. O. Topping, D. R. Glowacki, J. P. Reid, *Chem. Sci.* **2020**, *11*, 2999–3006.
[64] B. E. Poling, J. M. Prausnitz, J. P. O'Connell, *The properties of gases and liquids*, 5th ed., McGraw-Hill, New York, NY, **2001**.
[65] S. H. Chen, F. Mallamace, C. Y. Mou, M. Broccio, C. Corsaro, A. Faraone, L. Liu, *Proc. Natl. Acad. Sci. USA* **2006**, *103*, 12974–12978.
[66] a) D. L. Bones, J. P. Reid, D. M. Lienhard, U. K. Krieger, *Proc. Natl. Acad. Sci. USA* **2012**, *109*, 11613–11618; b) H. J. Tong, J. P. Reid, D. L. Bones, B. P. Luo, U. K. Krieger, *Atmos. Chem. Phys.* **2011**, *11*, 4739–4754.
[67] J. F. Davies, K. R. Wilson, *Anal. Chem.* **2016**, *88*, 2361–2366.
[68] T. C. Preston, J. F. Davies, K. R. Wilson, *Phys. Chem. Chem. Phys.* **2017**, *19*, 3922–3931.
[69] a) B. Nozière, C. Baduel, J.-L. Jaffrezo, *Nat. Commun.* **2014**, *5*, 3335; b) C. R. Ruehl, J. F. Davies, K. R. Wilson, *Science* **2016**, *351*, 1447–1450; c) H. C. Boyer, C. S. Dutcher, *J. Phys. Chem. A.* **2017**, *121*, 4733–4742.
[70] H. C. Boyer, B. R. Bzdek, J. P. Reid, C. S. Dutcher, *J. Phys. Chem. A.* **2017**, *121*, 198–205.
[71] B. R. Bzdek, J. P. Reid, J. Malila, N. L. Prisle, *Proc. Natl. Acad. Sci. USA* **2020**, *117*, 8335–8343.
[72] A. Hibara, M. Nonaka, M. Tokeshi, T. Kitamori, *J. Am. Chem. Soc.* **2003**, *125*, 14954–14955.
[73] T. Endo, K. Ishikawa, M. Fukuyama, M. Uraoka, S. Ishizaka, A. Hibara, *J. Phys. Chem. C* **2018**, *122*, 20684–20690.
[74] M. D. Summers, J. P. Reid, D. McGloin, *Opt. Express* **2006**, *14*, 6373–6380.
[75] D. McGloin, K. Dholakia, *Contemp. Phys.* **2005**, *46*, 15–28.
[76] J. S. Walker, A. E. Carruthers, A. J. Orr-Ewing, J. P. Reid, *J. Phys. Chem. Lett.* **2013**, *4*, 1748–1752.
[77] a) D. McGloin, *Philos. Trans. A Math. Phys. Eng. Sci.* **2006**, *364*, 3521–3537; b) A. E. Carruthers, J. P. Reid, A. J. Orr-Ewing, *Opt. Express* **2010**, *18*, 14238–14244; c) A. E. Carruthers, J. S. Walker, A. Casey, A. J. Orr-Ewing, J. P. Reid, *Phys. Chem. Chem. Phys.* **2012**, *14*, 6741–6748.
[78] M. I. Cotterell, B. J. Mason, T. C. Preston, A. J. Orr-Ewing, J. P. Reid, *Phys. Chem. Chem. Phys.* **2015**, *17*, 15843–15856.
[79] a) J. W. Cremer, K. M. Thaler, C. Haisch, R. Signorell, *Nat. Commun.* **2016**, *7*, 10941; b) J. W. Cremer, P. A. Covert, E. A. Parmentier, R. Signorell, *J. Phys. Chem. Lett.* **2017**, *8*, 3398–3403; c) M. E. Diveky, S. Roy, J. W. Cremer, G. David, R. Signorell, *Phys. Chem. Chem. Phys.* **2019**, *21*, 4721–4731.
[80] J. W. Lu, A. M. Rickards, J. S. Walker, K. J. Knox, R. E. Miles, J. P. Reid, R. Signorell, *Phys. Chem. Chem. Phys.* **2014**, *16*, 9819–9830.
[81] a) Z. Gong, Y. L. Pan, C. Wang, *Rev. Sci. Instrum.* **2016**, *87*, 103104; b) V. G. Shvedov, A. S. Desyatnikov, A. V. Rode, W. Krolikowski, Y. S. Kivshar, *Opt. Express* **2009**, *17*, 5743–5757.
[82] a) B. Redding, Y. L. Pan, *Opt. Lett.* **2015**, *40*, 2798–2801; b) Y.-L. Pan, C. Wang, S. C. Hill, M. Coleman, L. A. Beresnev, J. L. Santarpia, *Appl. Phys. Lett.* **2014**, *104*; c) B. Redding, S. C. Hill, D. Alexson, C. Wang, Y. L. Pan, *Opt. Express* **2015**, *23*, 3630–3639.

[83] a) V. G. Shvedov, A. V. Rode, Y. V. Izdebskaya, A. S. Desyatnikov, W. Krolikowski, Y. S. Kivshar, *Phys. Rev. Lett.* **2010**, *105*, 118103; b) V. G. Shvedov, C. Hnatovsky, A. V. Rode, W. Krolikowski, *Opt. Express* **2011**, *19*, 17350–17356; c) V. G. Shvedov, C. Hnatovsky, N. Shostka, A. V. Rode, W. Krolikowski, *Opt. Lett.* **2012**, *37*, 1934–1936.
[84] Y. L. Pan, S. C. Hill, M. Coleman, *Opt. Express* **2012**, *20*, 5325–5334.
[85] a) N. Eckerskorn, R. Bowman, R. A. Kirian, S. Awel, M. Wiedorn, J. Küpper, M. J. Padgett, H. N. Chapman, A. V. Rode, in *SPIE Nanoscience +Engineering* (Eds.: K. Dholakia, G. C. Spalding), **2015**, p. 95480H; b) N. Eckerskorn, L. Li, R. A. Kirian, J. Kupper, D. P. De Ponte, W. Krolikowski, W. M. Lee, H. N. Chapman, A. V. Rode, *Opt. Express* **2013**, *21*, 30492–30499; c) N. Eckerskorn, R. Bowman, R. A. Kirian, S. Awel, M. Wiedorn, J. Küpper, M. J. Padgett, H. N. Chapman, A. V. Rode, *Phys. Rev. Appl.* **2015**, *4*.
[86] a) M. L. Good, in *Technical Report No. UCRL-4146*, University of California Radiation Laboratory, **1953**; b) W. H. Hartung, C. T. Avedisian, *Proc. Math. Phys. Eng. Sci.* **1992**, *437*, 237–266.
[87] M. Tona, M. Kimura, *Rev. Sci. Instrum.* **2004**, *75*, 2276–2279.
[88] B. S. Vaughn, P. J. Tracey, A. J. Trevitt, *RSC Adv.* **2016**, *6*, 60215–60222.
[89] a) S. S. Steimer, U. K. Krieger, Y.-F. Te, D. M. Lienhard, A. J. Huisman, B. P. Luo, M. Ammann, T. Peter, *Atmos. Meas. Tech.* **2015**, *8*, 2397–2408; b) J. Dou, B. Luo, T. Peter, P. A. Alpert, P. Corral Arroyo, M. Ammann, U. K. Krieger, *J. Phys. Chem. Lett.* **2019**, *10*, 4484–4489.
[90] a) M. Y. Choi, C. K. Chan, *J. Phys. Chem. A* **2005**, *109*, 1042–1048; b) M. I. Jacobs, J. F. Davies, L. Lee, R. D. Davis, F. Houle, K. R. Wilson, *Anal. Chem.* **2017**, *89*, 12511–12519.
[91] A. W. Birdsall, U. K. Krieger, F. N. Keutsch, *Atmos. Meas. Tech.* **2018**, *11*, 33–47.
[92] a) Y.-H. Zhang, C. K. Chan, *J. Phys. Chem. A* **2000**, *104*, 9191–9196; b) C. Peng, C. K. Chan, *Atmos. Environ.* **2001**, *35*, 1183–1192; c) C. Peng, M. N. Chan, C. K. Chan, *Environ. Sci. Technol.* **2001**, *35*, 4495–4501; d) M. Y. Choi, C. K. Chan, *Environ. Sci. Technol.* **2002**, *36*, 2422–2428; e) M. Y. Choi, C. K. Chan, *J. Phys. Chem. A* **2002**, *106*, 4566–4572; f) M. N. Chan, C. K. Chan, *Environ. Sci. Technol.* **2003**, *37*, 5109–5115; g) Y.-H. Zhang, C. K. Chan, *J. Phys. Chem. A* **2003**, *107*, 5956–5962; h) Y.-H. Zhang, M. Y. Choi, C. K. Chan, *J. Phys. Chem. A* **2004**, *108*, 1712–1718; i) M. N. Chan, M. Y. Choi, N. L. Ng, C. K. Chan, *Environ. Sci. Technol.* **2005**, *39*, 1555–1562; j) M. N. Chan, A. K. Y. Lee, C. K. Chan, *Environ. Sci. Technol.* **2006**, *40*, 6983–6989; k) A. K. Y. Lee, C. K. Chan, *Atmos. Environ.* **2007**, *41*, 4611–4621; l) M. N. Chan, C. K. Chan, *Atmos. Environ.* **2007**, *41*, 4423–4433; m) T. Y. Ling, C. K. Chan, *Environ. Sci. Technol.* **2007**, *41*, 8077–8083; n) M. N. Chan, S. M. Kreidenweis, C. K. Chan, *Environ. Sci. Technol.* **2008**, *42*, 3602–3608; o) T. Y. Ling, C. K. Chan, *J. Geophys. Res.* **2008**, *113*; p) M. C. Yeung, A. K. Y. Lee, C. K. Chan, *Aerosol Sci. Technol.* **2009**, *43*, 387–399; q) L. P. Chan, A. K. Y. Lee, C. Chan, *Environ. Sci. Technol.* **2010**, *44 1*, 257–262.
[93] a) M. Y. Choi, C. K. Chan, Y.-H. Zhang, *J. Phys. Chem. A* **2004**, *108*, 1133–1138; b) M. Y. Choi, C. K. Chan, *J. Phys. Chem. A* **2005**, *109*, 1042–1048.
[94] A. K. Y. Lee, C. K. Chan, *J. Phys. Chem. A* **2007**, *111*, 6285–6295.
[95] K. A. Nadler, P. Kim, D. L. Huang, W. Xiong, R. E. Continetti, *Phys. Chem. Chem. Phys.* **2019**, *21*, 15062–15071.
[96] a) J. F. Davies, A. E. Haddrell, J. P. Reid, *Aerosol Sci. Technol.* **2012**, *46*, 666–677; b) C. Heinisch, J. B. Wills, J. P. Reid, T. Tschudi, C. Tropea, *Phys. Chem. Chem. Phys.* **2009**, *11*, 9720–9728; c) J. F. Davies, A. E. Haddrell, A. M. J. Rickards, J. P. Reid, *Anal. Chem.* **2013**, *85*, 5819–5826.
[97] a) F. K. A. Gregson, J. F. Robinson, R. E. H. Miles, C. P. Royall, J. P. Reid, *J. Phys. Chem. B* **2020**, *124*, 6024–6036; b) S. Ingram, G. Rovelli, Y.-C. Song, D. Topping, C. S. Dutcher, S. Liu, L. Nandy, M. Shiraiwa, J. P. Reid, *J. Phys. Chem. A* **2021**; c) J. F. Davies, A. E. Haddrell, R. E. H. Miles, C. R. Bull, J. P. Reid, *J. Phys. Chem. A* **2012**, *116*, 10987–10998; d) G. Rovelli, R. E. H. Miles, J. P. Reid, S. L. Clegg, *J. Phys. Chem. A* **2016**, *120*, 4376–4388; e) A. Marsh, R. E. H. Miles, G. Rovelli, A. G. Cowling, L. Nandy, C. S. Dutcher, J. P. Reid, *Atmos. Chem. Phys.* **2017**, *17*, 5583–5599; f) G. Rovelli, R. E. H. Miles, J. P. Reid, S. L. Clegg, *Atmos. Chem. Phys.* **2017**, *17*, 4369–4385; g) A. Marsh, G. Rovelli, R. E. H. Miles, J. P. Reid, *J. Phys. Chem. A* **2019**, *123*, 1648–1660; h) F. K. A. Gregson, M. Ordoubadi, R. E. H. Miles, A. E. Haddrell, D. Barona, D. Lewis, T. Church, R. Vehring, J. P. Reid, *Phys. Chem. Chem. Phys.* **2019**, *21*, 9709–9719; i) F. K. A. Gregson, J. F. Robinson, R. E. H. Miles, C. P. Royall, J. P. Reid, *J. Phys. Chem. B* **2019**, *123*, 266–276; j) N. E. Rothfuss, A. Marsh, G. Rovelli, M. D. Petters, J. P. Reid, *J. Phys. Chem. Lett.* **2018**, *9*, 3708–3713; k) Y. Y. Su, R. E. H. Miles, Z. M. Li, J. P. Reid, J. Xu, *Phys. Chem. Chem. Phys.* **2018**, *20*, 23453–23466; l) S. S. Petters, T. G. Hilditch, S. Tomaz, R. E. H. Miles, J. P. Reid, B. J. Turpin, *ACS Earth and Space Chemistry* **2020**, *4*, 741–749.
[98] J. Archer, J. S. Walker, F. K. A. Gregson, D. A. Hardy, J. P. Reid, *Langmuir* **2020**, *36*, 12481–12493.
[99] a) W.-P. Peng, Y.-C. Yang, M.-W. Kang, Y. T. Lee, H.-C. Chang, *J. Am. Chem. Soc.* **2004**, *126*, 11766–11767; b) W.-P. Peng, Y.-C. Yang, M.-W. Kang, Y.-K. Tzeng, Z. Nie, H.-C. Chang, W. Chang, C.-H. Chen, *Angew. Chem. Int. Ed.* **2006**, *45*, 1423–1426; *Angew. Chem.* **2006**, *118*, 1451–1454; c) W.-P. Peng, H.-C. Lin, H.-H. Lin, M. Chu, A. L. Yu, H.-C. Chang, C.-H. Chen, *Angew. Chem. Int. Ed.* **2007**, *46*, 3865–3869; *Angew. Chem.* **2007**, *119*, 3939–3943.
[100] M. O. Fernandez, R. J. Thomas, N. J. Garton, A. Hudson, A. Haddrell, J. P. Reid, *Journal of The Royal Society Interface* **2019**, *16*, 20180779.
[101] M. B. Hart, V. Sivaprakasam, J. D. Eversole, L. J. Johnson, J. Czege, *Appl. Opt.* **2015**, *54*, F174.
[102] a) V. Sivaprakasam, M. B. Hart, V. Jain, J. D. Eversole, *Opt. Express* **2014**, *22*, 18966; b) V. Sivaprakasam, M. B. Hart, J. D. Eversole, *J. Phys. Chem. C* **2017**, *121*, 22326–22334.
[103] A. Valenzuela, F. Chu, A. E. Haddrell, M. I. Cotterell, J. S. Walker, A. J. Orr-Ewing, J. P. Reid, *J. Phys. Chem. A* **2021**, *125*, 394–405.
[104] J.-y. Kohno, T. Higashiura, T. Eguchi, S. Miura, M. Ogawa, *J. Phys. Chem. B* **2016**, *120*, 7696–7703.
[105] C. N. Yeh, H. Huang, A. T. O. Lim, R. H. Jhang, C. H. Chen, J. Huang, *Nat. Commun.* **2019**, *10*, 422.
[106] I. Hussain, A. Hussain, A. Ahmad, H. Rahman, M. F. Alajmi, F. Ahmed, S. Amir, in *Graphene-Based Nanotechnologies for Energy and Environmental Applications* (Eds.: M. Jawaid, A. Ahmad, D. Lokhat), Elsevier, **2019**, pp. 241–266.
[107] a) W. Gao, G. Wu, M. T. Janicke, D. A. Cullen, R. Mukundan, J. K. Baldwin, E. L. Brosha, C. Galande, P. M. Ajayan, K. L. More, A. M. Dattelbaum, P. Zelenay, *Angew. Chem. Int. Ed.* **2014**, *53*, 3588–3593; *Angew. Chem.* **2014**, *126*, 3662–3667; b) F. Yang, M. Zhao, Z. Wang, H. Ji, B. Zheng, D. Xiao, L. Wu, Y. Guo, *RSC Adv.* **2014**, *4*, 58325–58328; c) Y. Ahn, H. Oh, Y. Yoon, W. K. Park, W. S. Yang, J.-W. Kang, *J. Environ. Chem. Eng.* **2017**, *5*, 3882–3894; d) Y. Yoon, H. Oh, Y. T. Ahn, M. Kwon, Y. Jung, W. K. Park, T. M. Hwang, W. S. Yang, J. W. Kang, *Catal. Today* **2017**, *282*, 77–85; e) T. Tomašević-Ilić, Đ. Jovanović, I. Popov, R. Fandan, J. Pedrós, M. Spasenović, R. Gajić, *Appl. Surf. Sci.* **2018**, *458*, 446–453.
[108] N. Leconte, J. Moser, P. Ordejón, H. Tao, A. Lherbier, A. Bachtold, F. Alsina, C. M. Sotomayor Torres, J.-C. Charlier, S. Roche, *ACS Nano* **2010**, *4*, 4033–4038.
[109] a) W.-J. Lan, C.-H. Chen, *Electrochim. Acta* **2015**, *180*, 1014–1022; b) C. C. Kuo, C. H. Chen, *Nanoscale* **2014**, *6*, 12805–12813.
[110] V. D. Ebajo, Jr., C. R. L. Santos, G. V. Alea, Y. A. Lin, C. H. Chen, *Sci. Rep.* **2019**, *9*, 15579.
[111] W. S. Hummers, R. E. Offeman, *J. Am. Chem. Soc.* **1958**, *80*, 1339–1339.
[112] C.-H. Chen, S. Hu, J.-F. Shih, C.-Y. Yang, Y.-W. Luo, R.-H. Jhang, C.-M. Chiang, Y.-J. Hung, *Sci. Rep.* **2017**, *7*, 3908.
[113] D. C. Marcano, D. V. Kosynkin, J. M. Berlin, A. Sinitskii, Z. Sun, A. Slesarev, L. B. Alemany, W. Lu, J. M. Tour, *ACS Nano* **2010**, *4*, 4806–4814.
[114] K. Hatakeyama, Y. Hakuta, J.-i. Sugiyama, Y. Shimizu, *Jpn. J. Appl. Phys.* **2019**, *58*, SIIA05.
[115] T. Du, A. S. Adeleye, T. Zhang, N. Yang, R. Hao, Y. Li, W. Song, W. Chen, *Environ. Sci.-Nano* **2019**, *6*, 2484–2494.
[116] F. J. Beltran, P. M. Alvarez, O. Gimeno, *Molecules* **2019**, *24*.
[117] a) J. Staehelin, J. Hoigne, *Environ. Sci. Technol.* **1982**, *16*, 676–681; b) J. Staehelin, J. Hoigne, *Environ. Sci. Technol.* **1985**, *19*, 1206–1213.
[118] a) J. Shang, L. Ma, J. Li, W. Ai, T. Yu, G. G. Gurzadyan, *Sci. Rep.* **2012**, *2*, 792; b) C. Galande, A. D. Mohite, A. V. Naumov, W. Gao, L. Ci, A. Ajayan, H. Gao, A. Srivastava, R. B. Weisman, P. M. Ajayan, *Sci. Rep.* **2011**, *1*, 85.
[119] a) P. J. Tracey, B. S. Vaughn, B. J. Roberts, B. L. J. Poad, A. J. Trevitt, *Anal. Chem.* **2014**, *86*, 2895–2899; b) J. Passig, J. Schade, M. Oster, M. Fuchs, S. Ehlert, C. Jäger, M. Sklorz, R. Zimmermann, *Anal. Chem.* **2017**, *89*, 6341–6345.
[120] a) Y. Sun, S. Yang, G. Zhao, Q. Wang, X. Wang, *Chem. Asian J.* **2013**, *8*, 2755–2761; b) J. Wang, Z. Chen, B. Chen, *Environ. Sci. Technol.* **2014**, *48*, 4817–4825.
[121] C. Zhang, L. Wu, D. Cai, C. Zhang, N. Wang, J. Zhang, Z. Wu, *ACS Appl. Mater. Interfaces* **2013**, *5*, 4783–4790.

Manuscript received: May 13, 2021
Accepted manuscript online: May 17, 2021
Version of record online: June 10, 2021